Dissertation

ASSOCIATION OF HEAVY METALS WITH SECONDARY IRON OXIDE MINERALS

Submitted by

Abdullah Al-Farraj

Department of Soil and Crop Sciences

In partial fulfillment of the requirements

For the Degree of Doctor of Philosophy

Colorado State University

Summer 2002

ProQuest Information and Learning Company
300 North Zeeb Road
P.O. Box 1346
Ann Arbor, MI 48106-1346

COLORADO STATE UNIVERSITY

June 11, 2002

WE HEREBY REMCOMMEND THAT THE DISSERTATION PREPARED UNDER OUR SUPERVISION BY ABDULLAH S. AL-FARRAJ ENTITLED **ASSOCIATION OF HEAVY METALS WITH SECONDARY IRON OXIDE MINERALS** BE ACCEPTED AS FULFILLING IN PART REQUIREMNTS FOR THE DEGREE OF DOCTOR OF PHILOSOPHY.

Committee on Graduate Work

K. A. Barbarick

Sally J. Sutton

Dan Hill

Advisor

Co-Adviser

K. A. Barbarick

Department Head, Acting

ABSTRACT OF DISSERTATION

ASSOCIATION OF HEAVY METALS WITH SECONDARY IRON OXIDE MINERALS

Retention of heavy metals by secondary iron oxide minerals is an important process in the soil environment. Therefore, knowledge of the mechanisms of heavy metals sorption on iron oxide minerals surfaces is necessary to predict the fate and mobility of heavy metals. This study examines the interactions of heavy metals (Pb, Zn, Cu, and Cd), with Fe oxide minerals in contaminated soil using selective extraction, EMP, MINTEQA2, and TEM with ED and EDX.

The soil samples were collected from a contaminated area near Leadville, CO. Total elemental concentration analysis of soil samples showed them to be contaminated with respect to Pb, Zn, Cu and Cd. Goethite was identified in the chemically untreated clay fraction for the 15-20 cm sample by using XRD. Amorphous and crystalline iron oxide minerals were identified by using TEM/ED and selective extractions. They ranged from 0.61 - 4.7% and 1.4 - 3.9% respectively.

Electron microprobe analysis demonstrated that the association of Pb with Fe is more pronounced than is Zn with Fe. Electron microprobe also revealed separate particles of Pb, Zn and Fe. These particles of Pb and Zn could be oxide, carbonate, sulfate or sulfide forms.

According to the results of MINTEQA2, the sequence of the adsorption of heavy metals to iron oxides is Pb> Cu> Zn> Cd. The modeled concentration of Pb associated with iron oxides was 38,100 mg kg^{-1}, for amorphous iron oxides. The analysis of five-selected iron oxide particles by using TEM/EDX gave an average Pb concentration of 42,900 mg kg^{-1} (Fe-oxides). Acidic ammonium oxalate in the darkness extraction gave 70,000 mg kg^{-1} (Fe-oxides). The AAOD reagent may over-estimate Pb associated with amorphous Fe-oxides, due to stripping of Pb adsorbed to crystalline Fe-oxides and also partial dissolution of Pb-rich particles not associated with Fe.

Our conclusions were that; the surface complexation models provide a fairly accurate prediction of the concentration of Pb bound to iron oxides. Also, surface adsorption was the most important mechanism of interaction of Pb with iron oxides in this soil. Selective extraction overestimated the concentration of Zn associated with Fe-oxides.

Abdullah S. Al-Farraj
Soil and Crop Sciences Department
Colorado State University
Fort Collins, CO 80523
Summer 2002

ACKNOWLEDGMENTS

I would like to express my thanks to Allah for His mercy during all my life and especially during the course of this study.

I especially thank my advisors, Dr. Eugene F. Kelly and Dr. Dean Heil, for their cooperation, encouragement, and support. Truly, their advice, guidance, assistance and efforts during my research and preparation of my dissertation are much appreciated.

Special thanks are due to my dissertation committee members, Dr. Kenneth A. Barbarick and Dr. Sally Sutton for their comments and helpful suggestions.

I would like to thank Dr. Susan Swapp in the Department of Geology and Geophysics at the University of Wyoming for her help with the electron microprobe analysis. I thank Dr Wendy Harrison in the Department of Geology and Geological Engineering at the Colorado School of Mines for her help with the analysis of X-ray diffraction. Also, I thank Dr. John Chandler and Kim in the Department of Colorado State University for their help with transmission electron microscope. I would like to express my thanks to Dr. Jim Self, manager of the Soil Testing Lab for his assistance with chemical analysis.

In addition, thank goes to those who assisted in this work. To, Geoffrey Upson, James Ippolito, Dr. Mohammad Al-Wabel and Colleen Green. Also, during my Ph.D. study, I was shown kindness and friendliness by everyone in Soil and Crop Science Department. I would like to thank all faculty members and staff of Soil and Crop Science Department.

Finally, I would like to thank my wife Haya and my children, Nourah, Asma, and Abdulrahman, for their patience and support. Special thanks due to my parents and my daughter Reem who are in Saudi Arabia, waiting for me to come back.

TABLE OF CONTENTS

LIST OF TABLES

LIST OF FIGURES

LIST OF APPINDECES

INTRODUCTION

Heavy Metals

Heavy metals are metals with a density more than 6 g cm^{-3}. Some heavy metals are essential in small quantities for life. They are called trace elements and include iron, copper and zinc. These metals in high concentrations may become toxic to living organisms (Alloway, 1990a). Thus, it is important to know the levels of these metals in soils, the mechanisms controlling their solubility, and the soil minerals which affect a metal's mobility and availability.

Because of industrialization, soil and water resources are at risk for contamination with heavy metals. In particular, the reclamation of polluted soils and evaluation of environmental risk necessitate a greater understanding about the interaction and association of heavy metals with soil components. Heavy metals interact with components of soil that are both organic and inorganic. Silicates, carbonates, phosphates, oxides and organic matter can all contribute to metal retention. In other words, they can mobilize or immobilize heavy metals (McBride et al., 1997; Kornicker et al., 1985; Parkman et al., 1998; Bradbury et al., 1999; and Ahnstrom and Parker, 1999). Tiller et al. (1984 a, b) found that heavy metals have a high affinity for naturally occurring solids in soils. Moreover, they found the reactions between heavy metals and solids – such as carbonates and oxides – are basically nonreversible. So, distribution of heavy metals between the solution and solid phases affects transport, bioavailability and toxicity in natural water (Fulghum et al., 1998). Under alkaline conditions many heavy metals

precipitate as hydroxides, carbonate, sulphates, phosphates and sulfides and their fate in the environment is generally unkown (Singh and Sadana, 1987).

Minerals occurring in nature seldom reside in the soil system in pure -crystalline phases (Stumm and Morgan, 1981). It is well known that ions can partition into various minerals phases during formation (Garrels and Christ, 1965) when they re-precipitate from soil solution.

Iron Oxide Minerals

Iron is present in most of the rocks in the earth's crust. Iron can be found in ferrous silicates, such as pyroxenes and amphiboles, sulphides, such as pyrite (FeS_2), and carbonates, such as siderite ($FeCO_3$) (Schwertmann and Cornell, 2000). The liberated iron from the weathering of primary iron minerals has a strong tendency to hydrolyze and form oxides. These resulting iron oxide minerals have a very low solubility at pH > 3. The solubility of iron oxides products range from 10^{-39}-10^{-44} (Schwertman and Taylor, 1989). The iron in oxide minerals could be partly replaced by other cations such as Al^{3+}, Mn^{3+}, Cr^{3+}, V^{3+}, Zn^{2+}, Cu^{2+}, and Pb^{4+}. The substitution of Al for Fe is common relative to other cations under natural conditions (Schwertmann and Cornell, 2000 and Schwertman and Taylor, 1989).

Iron oxide minerals are widespread in nature and are present in many soils of differing geologic and climatic conditions. They are generally associated with the clay size fraction in soils and have a strong influence on soil physical and chemical behavior (Schwertman and Taylor, 1989).

There are eight iron oxide minerals that have been recognized in soils that are

common. They include, but are not limited to goethite (α FeOOH), hematite (α Fe_2O_3), lepidocrocite (γ FeOOH), maghemite (γ Fe_2O_3), ferrihydrite ($Fe_5(O_4H_3)_3$), magnetite (Fe_3O_4), akaganeite (β FeOOH) and feroxyhyte (δ' FeOOH).

The dissolution and re-precipitation of iron oxide minerals in soils is conditioned by other soil properties such as pH, Eh, temperature and water activity (Schwertman and Taylor, 1989).

Iron oxides have an important role in the immobilization of heavy metals because of their high affinity for cationic polyvalent metals (Sauve et al., 2000). Jenne (1968) found that the hydrous oxides of Fe and Mn, rather than the clay minerals, have the dominant control on the fixation of these metals. Fuller et al. (1976) maintained that the percentage of free iron oxides is one of the most important factors for estimating an element's migration in the soil profile. For example, Brennan and Lindsay (1996) concluded that the activities of Zn, Cd and Pb are controlled by equilibrium between amorphous iron oxides (Fe_3O_4) and pyrite (FeS_2).

The chemical nature of the soil affects the solubility of heavy metals (Cavallaro and McBride, 1978). In general, acid soils were less able to retain the Cu and Cd than neutral soils. Their results support the findings that precipitation occurs in calcareous sub-soils. McBride et al. (1997) concluded that at pH < 7, hydroxides and carbonates of Cu and Mn were not involved in metal retention in the soil.

Chen et al. (1999) found that trace elements correlated better with total Fe and Al than with CEC. These data suggest that both total Fe and Al, even at low concentrations are significant in controlling heavy metal concentrations in some soils, Tiller et al. (1984 a, b) suggested that at low concentrations of heavy metals, adsorption-desorption

equilibrium is likely to control their concentrations in soil solution. On the other side, precipitation-dissolution reactions are important only at higher metal concentration.

OBJECTIVES

In this study I will investigate the interactions of heavy metals (Pb, Zn, Cu, and Cd) with Fe oxide minerals in contaminated soil. The following objectives guided my dissertation research: 1) To determine the forms of iron oxide minerals in soil; 2) To compare the relative behavior of Pb, Zn, Cu and Cd with respect to iron oxide minerals; 3) To determine the effects of various iron oxide minerals on adsorption of these metals.

RESEARCH QUESTIONS

1) What are the primary mechanisms of metal fixation to Fe oxides in a soil which has been polluted with acid mine wastes?.

2) Do surface complexation models provide an accurate prediction of the concentration of heavy metals bound to iron oxide minerals in soil?

3) Do amorphous Fe oxides contain higher concentrations of heavy metals than crystalline Fe oxides in soils?.

LITERATURE REVIEW

Heavy Metals Content in Soil

Total concentration of heavy metals in soils ranges between 2-200 ppm of Pb; 10-300 ppm of Zn; 2-100 ppm of Cu; and 0.01-0.7 ppm of Cd (Lindsay, 1979). The total content of these metals in contaminated soils differ widely according to the sources of the contamination (Alloway, 1990a).

Solubility of Minerals and Solid Forms of Heavy Metals in Soil

Heavy metals are present in soils both as dissolved species in solution and as solid phase compounds. Heavy metals form many mixed minerals in combination with carbonate, sulfate, oxide and hydroxide (Lindsay, 1979). Heavy metals may be found in soil solution, on exchange sites of soil minerals and organic matter, or adsorbed onto soil mineral surfaces (McBride, 1989). The precipitation of heavy metals may occur in cases where either very high concentrations of metals or certain anions or ligands are present (Kookana et al., 1999).

Lead is a widespread soil contaminant. It has a long residence time compared to most other pollutants. Therefore, its compounds tend to accumulate in soils (Davies, 1990). Since the partial pressure of CO_2 in soil is generally higher than that of the atmosphere, cerussite ($PbCO_3$) is the stable mineral in soils. Reducing condition makes $Pb(OH)_2$ the stable phase (Lindsay, 1979). Santillan-Medrano and Jurinak (1975) suggested that the solubility of lead might be regulated by phosphate in noncalareous

soils, whereas $PbCO_3$ could be important in calcareous soil. The major forms of lead ions, in aqueous solution, are Pb^{2+} and $PbOH^+$ below pH 8.0 (Lindsay, 1979).

The free ion of Zn^{2+} is a predominant species in solutions at values of pH $\leq$ 7.7, while $ZnOH^+$ is dominant above pH 7.7. The specific minerals that control Zn solubility in soils are not well understood. Franklinite ($ZnFe_2O_4$) in equilibrium with Fe^{3+} oxide could be that mineral (Lindsay, 1979). McBride and Blasiak (1979) found adsorption on permanent charge sites of clays, or complexation with organic matter could not account for the apparent fixation of Zn^{2+} in a none-exchangeable form in the pH range of 5-7. They suggested that nucleation of Zn hydroxide on clay mineral surfaces may have produced the strongly pH-dependent retention in the soil.

The soil Cd mineral is more stable than other minerals of Cd for pH $\leq$ 7.84. Depending on $CO_{2(g)}$, octavite ($CdCO_3$) controls Cd^{2+} activity at values of pH $\geq$ 7.84. The free ion Cd^{2+} is more likely to be adsorbed on the surface of soil solids than other species (Lindsay, 1979 and Alloway, 1990b). Holm et al. (1996) concluded that precipitation of $CdCO_3$ is not very likely to occur except under very extreme conditions. Therefore, Cd concentrations in calcareous soils are controlled primarily by sorption processes.

The least soluble form of copper is soil-Cu. Below a redox value of pe+pH = 14.89, cuprous ferrite ($Cu_2Fe_2O_4$) in equilibrium with soil-Fe becomes the stable mineral of copper depending on availability of other anions. Also, under reducing conditions, Cu occurs as the native metal when sulfide is unavailable. The major forms of copper in aqueous solution are Cu^{2+} and $Cu(OH)^\circ_2$ for acid soils and neutral and alkaline soils respectively (Lindsay, 1979 and Baker, 1990).

Wu et al. (1999) studied sorption and desorption of Cu on soil clay components. They found, after removing organic matter, the fine clay (<0.02 μm) exhibited higher Cu retention than did the coarse clay (0.2-2.0 μm). They noticed that Cu appears to be specifically sorbed on the surfaces of silicate clays in excess of that which variable charge sites can account for. They suggested that Fe oxides might coat lateral surfaces of layer silicates, blocking access of Cu to potential sorption sites. McBride and Blasiak (1979) noticed that an organic complexation mechanism controls Cu.

Factors Affecting Heavy Metals in Soil

There are several factors that determine whether heavy metals will remain in soil solution. These are: 1) concentration of the metal; 2) the competing cations; 3) concentration of all ligands; 4) pH and redox potential; and 5) nature and amount of sorption sites associated with the solid phase (Harmsen, 1977). These processes, which control the partitioning of metals in soil, involve several types of reactions. These are: 1) Adsorption and desorption; 2) Precipitation and solubilization; 3) Surface complex formation; 4) Surface precipitation; 5) Ion exchange; 6) Penetration of the crystal structure of minerals; and 7) Biological mobilization and immobilization (Chao, 1984).

It is often assumed that the removal of an ion from a solution by an adjacent solid phase takes place by an adsorption mechanism. However, there are conditions under which this assumption may not be acceptable. Therefore, it is necessary to determine what sorption process has occurred, e.g., whether surface precipitation or adsorption is responsible for the sorption of an ion from the aqueous phases. Tewari and Lee (1975) observed surface precipitation of $Co(OH)_2$ at high surface coverage of the metal and relatively high pH. Schenck et al. (1983) found evidence of surface precipitation of

cobalt on goethite. Also, Harvey and Linton (1984) observed similar results of zinc sorption on hydrous ferric oxide. McBride et al. (1984) showed that predominate sorption process of Cu^{2+} onto gibbsite was surface precipitation as pH and coverage increased.

At low concentrations of cations, surface complexation tends to be the dominant sorption mechanism. Harvey and Linton (1984) and Farley et al. (1985) indicated that the contribution of surface precipitation increases with increases in the concentrations of heavy metals. Surface precipitation is an ideal solid solution of the surface phase (Farley et al., 1985 and Dzombak and Morel, 1986). Moreover, surface precipitation becomes the dominant sorption mechanism when the surface sites become saturated at very high concentrations. In the surface precipitation concept, a new hydroxide surface forms. Hydroxide precipitates may develop on the surface of iron oxide minerals before their formation in the bulk solution. Therefore, they contribute to total apparent sorption (Dzombak and Morel, 1990). Dzombak and Morel (1986) suggested that surface precipitation was the cause of the slow rate of accumulation onto hydrous ferric oxide at high concentrations of Cd.

Sposito (1989) defines co-precipitation as the simultaneous precipitation of a chemical element with other elements by any mechanism and at any rate. The three widespread types of co-precipitation are inclusion, adsorption and solid solution formation.

Adsorption of Heavy Metals in Soil

When a metal cation adsorbs onto a mineral surface it can be either inner sphere or outer sphere complexation. If a water molecule is located between the surface

functional group and the bound metal ion, the surface complex is defined as outer sphere. Similarly, if the water molecule is not present between the sorbed ion and the surface, the surface complex is described as an inner sphere (Sposito, 1989). Furthermore, inner sphere complexes could be a monodentate or a bidentate inner sphere according to the number of bonds that attach the metal to the surface. A monodentate inner sphere complex incorporates a single bond between the metal ion and surface oxygen while a bidentate complex has two direct bonds of the metal to separate surface oxygens (Hayes, 1987).

Influence of Iron Oxide Minerals on the Behavior of Heavy Metals

Brummer et al. (1983) studied adsorption-desorption and/or precipitation-dissolution processes of Zn in soils. They found that for pHs below 7, the concentrations of Zn in equilibrium solutions with soil clay and whole soil are determined only by adsorption-desorption reactions. In contrast, precipitation of Zn may appear at neutral to alkaline pH values. Also, they found that the adsorption capacity for specifically adsorbed Zn in $CaCO_3$-buffered systems is 0.44 μmol g^{-1} of $CaCO_3$, 44 μmol g^{-1} of bentonite, 842 μmol g^{-1} of humic acid, 1190 μmol g^{-1} of Fe-oxide, 1310 μmol g^{-1} of Al-oxide, and 1540 μmol g^{-1} of δ-MnO_2. Therefore, Mn-, Fe-, and Al- oxides and humic substances are important for the retention of Zn in soils containing carbonates. This indicates the special role of these components in limiting precipitation reactions.

Shuman (1988) found that Fe oxides are important in Zn adsorption. However, removing them increased Zn adsorption in some soils and decreased it in others. Saeed and Fox (1979) found that adsorption of Zn increases with additions of phosphate to soils by increasing the negative charge on Fe and Al oxide systems.

Santillan-Medrano and Jurinak (1975) found the solubility of Cd and Pb is reduced with increasing pH. Cd was found to be more mobile. Its precipitation in soil was not effective in decreasing its mobility. Therefore, it was suggested that soils hold this relatively soluble metal by adsorption or exchange. Cadmium adsorption depends on chemical and mineralogical characteristics of the soils and the composition of the soil solution (Pardo, 1997). Papadopoulos and Rowell (1988) obtained the same results. $Cd(OH)_{2(s)}$ is unlikely to form in nature because of its instability and high solubility (Lindsay, 1979).

Cavallaro and McBride (1984) investigated the influence of soil oxides in soil clays from an acid New York soil on Cu and Zn sorption and fixation. They concluded that microcrystalline and noncrystalline oxides in the clay fraction of the soil provide reactive surfaces for the chemisorption of Cu and Zn. At a low pH, adsorption to these surfaces may be the dominant mechanism of heavy metal immobilization, especially in the subsoil horizons. They also found that microcrystalline oxides were important for Cu sorption, while the crystalline oxides appear to have a significant role in Zn adsorption. Moore et al. (1988) and Karlsson et al. (1988) noticed that Zn may exist primarily in the oxide fraction in acid soils.

Fu et al. (1991) found that adsorption of Cd and Cu increased with increasing pH because of hydrolysis of metal cations and/or variable charge sites on MnO_2. Their results show that the affinity of MnO_2 for Cu is greater than that for Cd. More over, MnO_2 has high adsorption capacities and high adsorption affinities for Cd and Cu even in acidic conditions.

Yarlagadda et al. (1995) characterized several heavy metal-contaminated soils

using a variety of techniques. They found Pb to be associated primarily with carbonate and the Fe-Mn oxide phases of the soil samples. Also, Cu was absorbed to be associated with carbonate, Fe-Mn oxide and organic fractions of the soils. The amount of Pb and Cu, which are held in the exchangeable form, was very low in their study.

Several researchers have found that most of the Pb was associated with the oxide fraction (Sposito et al., 1982; Chlopecka, 1993; and Ramos et al., 1994). Goldberg (1954) and Krauskopf (1956) reported that iron and manganese oxide minerals are known to scavenge trace elements from solution.

Goldberg et al. (1996) found adsorption of Mo on both Al and Fe oxides exhibited a maximum at low pH extending to about pH 4-5. Also, Mo adsorption on clay minerals exhibited a peak near pH 3 and then decreased rapidly with increasing pH until adsorption was virtually zero near pH 7. The amount of Mo adsorption on clay increased in the order: kaolinite < illite < montmorillonite.

Levy et al. (1992) studied the distribution and partitioning of trace metals in contaminated soils near Leadville, Colorado. They found that copper was predominantly associated with organic matter. However, Pb, Cd and Zn were mainly bound to Fe and Mn oxides.

Surface Complexation Models

During the last three decades, surface complexation models have been developed to model the adsorption of ions at the mineral/aqueous interface. These models assume that minerals have surface functional groups which are also referred to as "sites." These sites can form complexes with the adsorbing species (Goldberg, 1995).

The Diffuse Layer Model (DLM) and the Triple Layer Model (TLM) are examples of surface complexation models (Goldberg, 1995). Dzombak (1986) and Dzombak and Morel (1986) used the DLM to model the adsorption of Cd at the hydrous iron oxide/aqueous interface. Dzombak and Morel (1987) have also demonstrated the DLM's effectiveness in simulating Cr removal by adsorption onto hydrous iron oxide.

Davis and his coworkers used the TLM to successfully model the adsorption behavior of metal ions, ligands and metal-ligand complexes at the oxide/aqueous interface (Davis et al., 1978; and Davis and Leckie, 1978a; 1978b; 1979; and 1980). The TLM was found adequate in modeling adsorption of ions on oxides suspended in seawater (Balistrieri and Murray, 1979; 1981; and 1982). Dzmobak and Morel (1990) found the single surface layer, two site surface complexation model was used with excellent results for sorption of the metal ions Co^{2+}, Ni^{2+}, Cd^{2+}, Zn^{2+}, Cu^{2+}, Pb^{2+} and Hg^{2+}.

The above literature review reveals that surface complexation models have been extensively studied. However, the application of these models to iron oxide minerals in soils has been very limited.

MATERIALS AND METHODS

Field Methods

The soil samples used for this study were collected in 1998 from Smith Ranch below California Gulch (Figure 1). Smith Ranch has received irrigation water from California Gulch which is contaminated by hydraulically transported mine tailings deposited in the early 1900s (Levy et al., 1992). The site of the samples is located on a small flood plain that has been subject to seasonal flooding. This soil is classified as Typic Cryaquoll. This contaminated site was chosen because of its high iron content. Also, it contained substantial accumulations of Cu, Cd, Pb, and Zn (Levy et al., 1992).

Soil samples were collected from four different depths, down to a maximum depth of 20 cm. These depths were 0-5, 5-10, 10-15 and 15-20 cm. The samples were mixed to ensure homogeneity, dried at room temperature and gently ground to pass through a 2 mm sieve. For this study, the first soil depth (0-5 cm) was not included.

Laboratory Methods

Clay Size Separation

For clay size separation, only physical dispersion was done as a pretreatment. After that, the solution was increased to a 2 L volume with distilled water. The suspension was stirred carefully with a hand stirrer for at least 1-2 min. After 7.5 h, the pipette was lowered carefully to 10 cm depth and the suspension of <2-μm clay in the

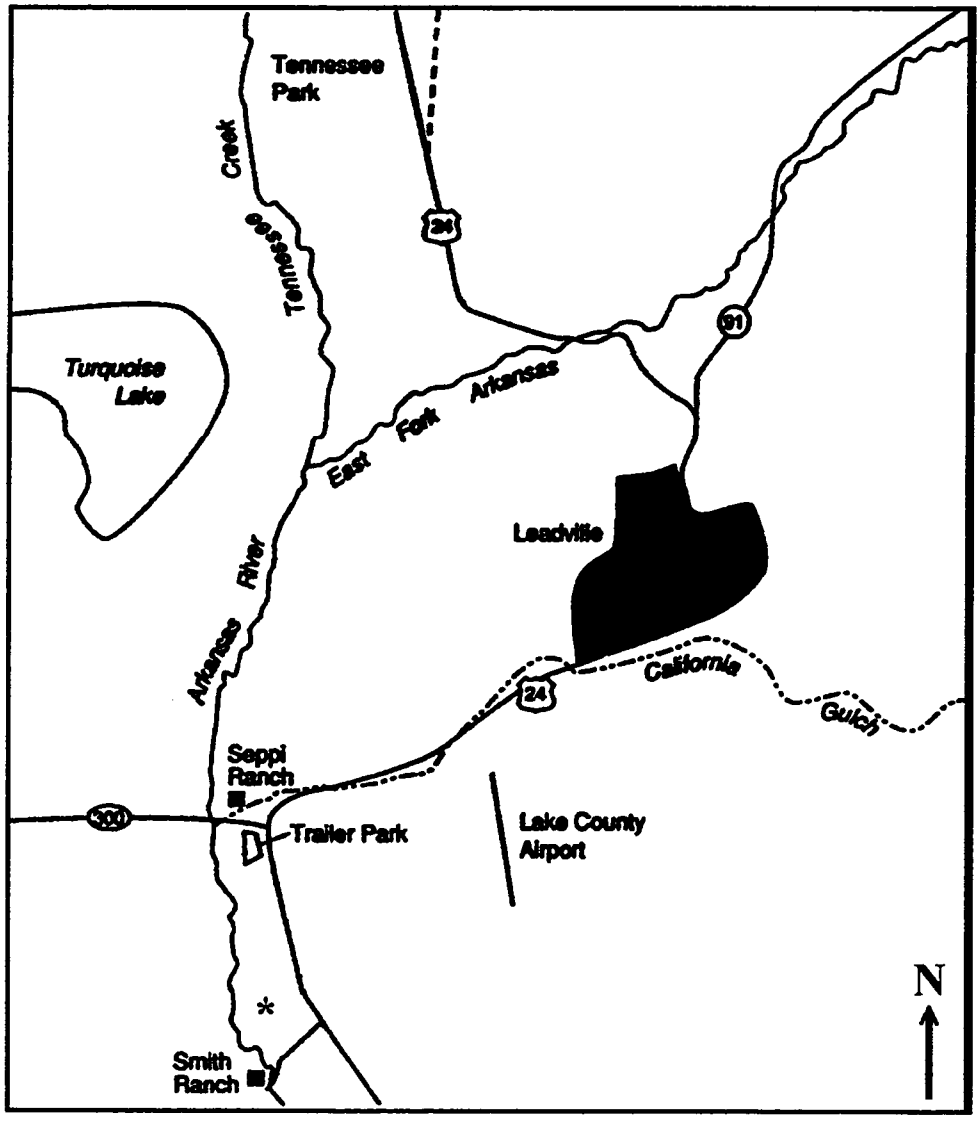

Fig. 1: Study site location (*) near Leadville, CO. (Levy et al., 1992).

cylinder was collected using a siphon. The last three steps were repeated many times to have nearly complete separation. Then the suspension of <2-μm clay was transferred to a group of 250-mL centrifuge tubes. A sufficient amount of NaCl was added to enhance the flocculation of particles. After the centrifugation, the supernatant was decanted. The sediment in the bottom of the tubes were transferred to a small flask and dried at room temperature. The suspension of >2-μm silts and sands was treated as clay suspension was minus the addition of NaCl.

Chemical Analyses

Soil samples, fractions of clay size particles and of silt and sand were digested with HNO_3-$HClO_4$-HF and analyzed for total elemental content by ICP-AES (Hossner, 1996). Soil pH was measured in distilled water extracts after equilibration for 24 h. The ratio of soil and distilled water was 1:2 (Thomas, 1996).

A LECO CHN analyzer determined the total carbon contents of the soil samples (TC). Soil organic matter was determined by multiplying the organic carbon concentration by 1.724 (Nelson and Sommers, 1996). Total inorganic carbon (TIC) contents were measured by using a gravimetric method (Loeppert and Suarez, 1996). Also, total organic carbon contents of soil samples were calculated as a difference between total carbon and total inorganic carbon. Particle size distribution was determined by the hydrometer method (Gee and Bauder, 1996).

Extraction of Iron Oxide Minerals

Procedures of selective extraction were not sequential. Each of these procedures is operationally defined as follows. For total free iron oxides, samples were extracted

with the citrate bicarbonate dithionite method (Loeppert and Inskeep, 1996). The acid ammonium oxalate in darkness method was performed to extract the amorphous iron oxide (Loeppert and Inskeep, 1996). Water-soluble and exchangeable iron were extracted by using magnesium chloride. For each sample, two observations were taken. Two blanks were run as well as the soil samples. After each extraction procedure, samples were centrifuged and the supernatant were collected. Concentrations of iron, lead, zinc, copper and other elements for all extractions were determined by Inductively Coupled Plasma – Atomic Emission Spectroscopy "ICP-AES" (Loeppert and Inskeep, 1996).

For water soluble metal concentrations, a sample of soil (10.0 g) was suspended in 20 ml of deionized water in a polypropylene centrifuge tube and shaken for 24 h. The soil suspension was centrifuged and the supernatant solution filtered through a 0.2 μm filter and acidified by using HNO_3.

MINERALOGICAL ANALYSES

Soil samples were treated chemically prior to particle size fractionation. Soluble salts and carbonates were removed by using the sodium acetate buffer method (Kunze and Dixon, 1994). Organic matter was removed by using NaOCl (Moore and Reynolds, 1997). Finally, free iron oxides were removed by using dithionite citrate-sodium bicarbonate (Kunze and Dixon, 1994).

After chemical treatment, soil suspensions were dispersed by a combination of chemical and physical methods using Na-hexametaphosphate. For samples that were only subject to physical dispersion, a 5 min mixing with a standard electrical mixer was performed (Gee and Bauder, 1996).

Soil samples were then separated into three size fractions. They are sand (2-0.05 mm), silt (0.05-0.002 mm), and clay (<0.002 mm) utilizing standard sedimentation procedures (Gee and Bauder, 1996 and Jackson, 1956).

All size fractions of soil were examined by using X-ray diffraction (XRD). Both the sand and silt sized fractions were analyzed using a random powder procedure; whereas clay sized materials were oriented by using the method of filter transfer (Moore and Reynolds, 1997). All size fractions from the 15-20 cm depth were separated mechanically and analyzed utilizing the random powder procedure. Samples of clay fractions were saturated by Mg and K and subjected to heating (K slides) and glycolation (Mg slides) procedures

Samples were subjected to XRD using CuKα (1.5406 A°) radiation (45 kV, 35 mA) on a Philips vertical goniometer in a range of 2° 2θ to 65° 2θ or from 2° 2θ to 30° 2θ (Colorado School Mines) (Whittig and Allardice, 1994).

For semi-quantitative percentages of clay minerals, the intensity of peaks from Mg-EG treatment at 10.0, 7.15, and 3.35Å for illite, kaolinite and quartz respectively were used. There was correction for quartz by subtracting 75% of the peak at 10.0Å. The percentage of vermiculite was calculated from the difference between the 14Å peak area of Mg-EG and the K-550°C treatments. The following equation was used for calculating the percentage of clay minerals:

$$\text{Weight \%} = 100 * (\text{Intensity/MIF})/\text{Sum}$$

where I is the integrated peak area; MIF is the mineral intensity factor; and Sum is the total of (I/MIF) for all minerals. The MIF were 1, 2.5, 4 and 5 for illite, kaolinite, quartz and vermiculite respectively (Klages and Hopper, 1982).

ELECTRON MICROPROBE ANALYSES

Preparation of Samples

To study the distribution of heavy metals in iron oxide minerals, samples of soil at depth 15-20 cm (<2.0 mm and chemically untreated clay fraction) were impregnated with plastic (Acrylimet epoxy, South Bay Technology, Inc., San Clemente, CA). Plastic boats (7 x 16 x 10 mm) were used for impregnation. Samples were left for 24 h at room temperature and at 138 kPa of pressure. The embedded samples were then removed from the plastic boats and affixed to glass slides. Then, the embedded soil samples were wet wheel-polished with an Exakt automated microgrinder using 800, 1200 and then 2000 grit polishing paper to produce a relief-free surface. Polished specimens of soils were coated with a thin layer of carbon in a vacuum evaporator (Kinney vacuum evaporator Model KDTG-3P) (Sawhney, 1986).

Analyses of Samples

A JEOL JXA-8900 Electron Microprobe analyzer (JEOL USA, Inc., Peabody, MA) at an accelerating voltage of 15 keV and a magnification between 244x and 1000x, was used to scan the above samples (University of Wyoming). Moreover, elemental analysis for some spots were obtained using wavelength dispersive X-rays during electron probe observations.

TRANSMISSION ELECTRON MICROSCOPE ANALYSIS

The micron and sub-micron sized particles affect many of the chemical and physical properties of soils. These small particles cannot be investigated by optical microscopy. A transmission electron microscope (TEM) provides two dimensional images of crystals ranging in size from a few nm to a few μm. Also, energy dispersive X-ray analysis (EDX) is useful in determining the chemical composition of the particles of minerals. A diluted suspension is necessary to prevent both a crowded grid and aggregation of particles, which causes difficulty for identification of crystal shapes and sizes (Gilkes, 1994).

Preparation of Soil Samples

The chemically untreated clay fraction was prepared at 64 mg L^{-1} dilution with deionized water. A few μl of that suspension was placed on a specimen grid coated with a perforated (holey) carbon supporting film and allowed to dry. For optimum imaging, the formvar film was removed from the grids by using chloroform. Procedures were adopted to maintain sample purity and avoid possible contaminants (Gilkes, 1994).

Preparation of Synthetic Iron Oxide Minerals

Synthetic goethite was prepared following the procedure of Schwertmann and Cornell (2000). Exactly 100 ml of 1 M $Fe(NO_3)_3$ solution was added rapidly with stirring to 180 ml of 5 M KOH solution. Immediately, the red brown suspension was diluted to 2 L with distilled water and held in a closed polyethylene flask at 70°C for 60 h. Glass vessels were avoided because some Si would be dissolved in strongly alkaline media.

The yellowish suspension was centrifuged, washed and dried. This procedure provides goethite with a surface area of 20 $m^2 g^{-1}$.

TEM/EDX Analysis of Pb concentration in Soil Fe oxide particles

Transmission electron micrographs were obtained using a JEOL 4000 FX electron microscope operated at 100 kV (Electron Microscopy Center Colorado State University). Five selected particles of soil sample (chemically untreated clay) were analyzed by energy-dispersive X-ray and data semi-quantitatively processed. Selected elements were Fe, Pb, Zn, Cu and Cd. Also, particles of synthetic goethite were imaged and ED patterns collected. Quantitative results are presented for Pb only. Copper could not be measured because the sample grid is constructed with Cu. Zinc was not quantified because the broad Cu peaks interfered with the primary Zn peak. The electron diffraction (ED) pattern was then focused and held only by beams originating from the chosen area. With ED, an electron beam can be strongly scattered by atoms and produce a diffracted beam. This diffracted beam can then be re-diffracted by a second set of planes. These diffracted electrons give direct crystallographic information (Williams and Carter, 1996).

For fine particles, such as usually investigated by TEM, the ratio of intensities of spectral lines for elements are related to the ratio of their concentrations in the particles (Williams and Carter, 1996). Therefore, the determination of the composition of the particles is achievable.

MODELING THE ADSORPTION OF HEAVY METALS BY IRON OXIDE MINERALS WITH MINTEQA2

Surface complexation models are chemical models that can describe adsorption reactions. There are several adsorption models (For example, the constant capacitance model, the diffuse layer model, the triple layer model, etc). Surface complexation models treat adsorption as a surface complexation reaction and accounts for the electrostatic potentials at the charged surface. The models differ in the following ways: 1) The types of surface species that are allowed within specific physical locations or layers extending away from the surface; and 2) The parameters of the electrostatic model that each employs. In all three models, a charge (σ) associated with the surface is assumed to be balanced by a charge (σ_d) associated with a diffuse layer of counterions. These charges are such that $\sigma + \sigma_d = 0$ (Allison et al., 1991 and Goldberg, 1995).

The Diffuse Layer Model

Stumm and coworkers proposed the diffuse layer model (DLM) (Stumm et al., 1970; and Huang and Stumm, 1973). Dzombak and Morel then developed it (1990). In the DLM, all specifically adsorbed ions contribute to the surface charge (σ) and two planes of charge represent the surface. The equations for the surface complexation reactions include acidity reactions, which are protonation and dissociation. The protonation reaction is written as the following:

$$=SOH + H^+ \leftrightarrows =SOH^{2+} \qquad 1$$

And the dissociation reaction is:

$$=SOH \leftrightarrows =SO^- + H^+ \qquad 2$$

where H^+ denotes a hydronium ion near the surface. SOH represents an acidically active surface site. This surface site can also exhibit binding with ions. For cations, it is assumed that high and low energy sites are present on the surface. Therefore, two intrinsic constants are required by the DLM. The surface reaction involving the divalent cation M^{2+} is written as:

$$=SOH + M^{m+} \leftrightarrows =SOM^{(m-1)} + H^+ \qquad 3$$

Fig. 2 A shows a theoretical structure of an oxide surface as represented by the DLM (Allison et al., 1991).

The input parameters for the DLM are the following:

1- The activities of soluble ions at equilibrium of the studied soil samples as shown in table 1. The activities were calculated as the using the following equation:

$$(i) = \gamma_i [i] \qquad 1$$

where i is a chemical species; (i) is its activity; [i] is its concentration; and γ_i is the activity coefficient, which was calculated as:

$$\text{Log } \gamma_i = -0.512 Z_i^2 \{[(I^{1/2})/(1+ I^{1/2})] - 0.3 I\} \qquad 2$$

where Z_i is the ion valence; and I is the ionic strength. And the following equation was used to calculate the ionic strength:

$$I = 1/2 \Sigma Z_i^2 [i] \qquad 3$$

where the sum is over all charged ions in solution.

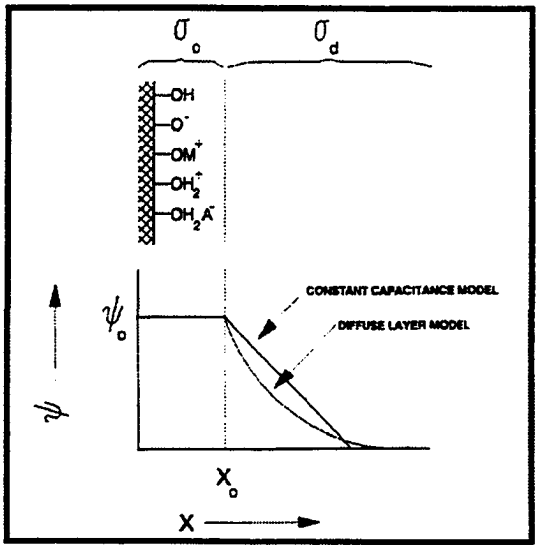

A

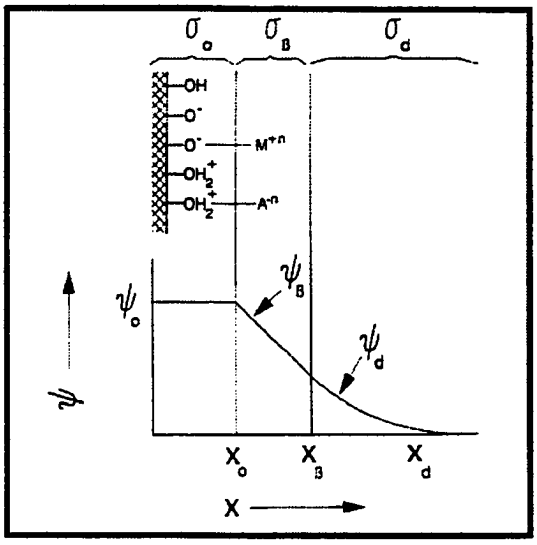

B

Fig. 2: Structure of the surface solution interface for the DLM (A) and for TLM (B) (After Allison et al., 1991).

Table 1: Input data used in modeling adsorption of metals to the amorphous iron oxide and goethite in the three soil horizons.

Element	05:10 cm	10:15 cm	15:20 cm
		Activity	
Ca	3.15E-05	6.93E-05	1.03E-04
Cd	2.79E-07	1.33E-07	1.31E-07
Cu	1.77E-06	6.06E-07	7.08E-07
K	1.79E-04	7.00E-05	6.64E-05
Mg	2.16E-04	5.39E-05	7.43E-05
Na	2.88E-05		
Pb	1.89E-06	2.25E-07	6.10E-07
Zn	4.20E-05	1.96E-05	2.06E-05
Cl	8.67E-05	2.25E-04	2.83E-04
pH	6.81	6.96	6.74

The concentrations of Ca, Cd, Cu, K, Mg, Na, Pb and Zn were taken from results of water soluble extraction. The concentration of Cl^- was assumed to be equal the total concentrations of above cations.

2- The concentration of amorphous iron oxide is assumed to be 1 g L^{-1}.

3- The surface site density is the total number of surface sites. Dzombak and Morel (1990) selected the arithmetic mean of the experimental ranges for amorphous Fe oxides, which are 0.005 moles $mole^{-1}$ of Fe (5.63×10^{-3} mole g^{-1}) for the high energy site density and 0.2 moles $mole^{-1}$ of Fe (2.25×10^{-3} mole g^{-1}) for the low energy sites.

4- The molecular weight of amorphous Fe-oxide is 89 based on the chemical formula FeOOH.

5- The specific surface area of amorphous iron oxides is assumed to be 600 m^2 g^{-1} (Dzombak and Morel, 1990).

6- Version 3.0 of MINTEQA2 includes a database for describing adsorption of the trace metals and the ligands onto two types of iron oxides with the DLM (Goldberg, 1995). This information is contained in the file feo-dlm.dbs.

The concentrations of metals in amorphous iron oxide and goethite were calculated as the following:

$$Me_{(mg)} / \text{Fe-oxide}_{(kg)} = [Me] * A.W. * 10^6 \qquad 4$$

where Me is the metal; [Me] is its sorbed concentration from the output of MINTEQA2 in units of mol L^{-1} (water); and A.W. is the atomic weight of the metal. The value was multiplied by 10^6 to provide units of mg of metal per kg of iron oxide.

The Triple Layer Model

The triple layer model is generally more complex than the DLM. In the TLM, the net surface charge is the sum of the charges associated with two adsorbing planes. The innermost of them (the o-plane) specifically adsorbs H^+ and OH^- and is characterized by charge σ_o. The other plane (β-plane) has a charge σ_β resulting from the adsorption of other ions. For inner sphere surface complexation reactions, the equations are similar for the DLM. The equations involving the divalent cation M^{2+} are written as:

$$=SOH + M^{m+} \leftrightarrows =SO^-M^{(m-1)} + H^+ \qquad 4$$

$$=SOH + M^{m+} + H_2O \leftrightarrows =SO^-MOH^{(m-1)} + 2H^+ \qquad 5$$

where splitting the surface complexes with dashes indicate outer sphere complexes. Fig. 2 B illustrates the structure of the surface solution interface for the TLM (Allison et al., 1991).

Many experimental studies of pure oxide systems indicate that these surface complexation models can predict the adsorption behavior of heavy metals in well-defined systems (Allison et al., 1991). Balistrieri and Murray (1982b) modeled the adsorption of heavy metals by goethite by using the TLM. Therefore, the adsorption of heavy metals (Cd, Cu, Pb and Zn) by amorphous iron oxide minerals and goethite in each of the three soil layers was modeled using the DLM and TLM, respectively.

The Input Parameters for the TLM are the Following:

1.The activities of soluble ions of the studied soil samples are summarized in Table 1.

2.The concentration of the on the solid is assumed to be 1 g L^{-1}.

3.The surface site density is the total number of exchangeable surface sites. This was determined by titration to pH 11 in 1 M NaCl and was equal to 4.25 x 10^{-6} moles m^{-2} (0.22 moles kg^{-1}) (Balistrieri and Murray, 1979).

4.The specific surface area of goethite as determined by N_2 adsorption and was found to be 51.8 m^2 g^{-1} (Balistrieri and Murray, 1983).

5.The formula weight of goethite is 89 based on the chemical formula FeOOH.

6. Based on the work of Stumm et al. (1970) and Davis and Leckie (1978a), the capacitance of the outer layer (C2) is set at 0.20 farads m^{-2}. The inner layer capacitance (C1) is set at 1.40 F m^{-2}.

7. The set of surface reactions and the intrinsic equilibrium are provided by Balistrieri and Murray (1982). The intrinsic equilibrium constants that were observed in the absence of an electric field were used instead of equilibrium constant because electrical double layer properties influence the rates of elementary reaction steps and equilibrium constants between solid and liquid phases. These reactions are:

$=SOH + H^+ \leftrightarrows =SOH^{2+}$	5.57	1
$=SOH \leftrightarrows =SO^- + H^+$	-9.52	2

$=SOH + Pb^{2+} \leftrightarrows =SO^{-}Pb^{+} + H^{+}$	-1.80	6
$=SOH + Pb^{2+} + H2O \leftrightarrows =SO^{-}PbOH + 2H^{+}$	-5.00	7
$=SOH + Zn^{2+} + H_2O \leftrightarrows =SO^{-}ZnOH + 2H^{+}$	-9.15	8
$=SOH + Cu^{2+} \leftrightarrows =SO^{-}Cu^{+} + H^{+}$	-3.00	9
$=SOH + Cu^{2+} + H_2O \leftrightarrows =SO^{-}CuOH + 2H^{+}$	-7.00	10

The intrinsic equilibrium constants for the above reactions were formulated in the following manner (for example, reaction 1):

$$K = \{(SOH^{2+})\,(H^{+})\}/\{(SOH)\,(H^{+})\,(e^{-\Psi oF/RT})\} \qquad 5$$

where the ( ) refers to the activity of the ion; $e^{-\Psi oF/RT}$ is an electrostatic or coulombic correction factor; F is the Faraday constant (9.6485×10^{4} C mol^{-1}); R is the ideal gas constant (8.3145 J K^{-1} mol^{-1}); T is the absolute temperature (K); and Ψ_o is the surface potential (V) (Allison et al., 1991).

RESULTS AND DISCUSSION

SOIL CHEMICAL PROPERTIES

Table 2 shows the concentrations of water-soluble metals from 1:2 soil:water extractions. The measurable concentrations in soil solution were generally low. The basic physicochemical properties of studied soil samples are summarized in table 3.

Table 4 shows the concentration of elements of soil samples at three depths compared to the average concentrations and the normal ranges in soils. All of these soil samples were contaminated with respect to Cd, Pb and Zn. And all depths, except for 10-15 cm, were contaminated with respect to Cu. Soil samples at depths 5-10 cm and 15-20 cm were contaminated with respect to B. Also, soil at depth 0-5 cm was contaminated with respect with Mo.

Total concentrations of Fe and Mn at 0-5, 5-10 and 15-20 cm depths were higher than the average concentration reported for other soils; however, they were less than the averages at the depth of 10-15 cm.

The soil at depths of 10-15 cm has the greatest sand content. This coincided with a low percentage of Cd, Pb, Zn, Cu, Mn and Fe. This is probably a result of the low clay content and negligible sorption by dominant quartz grains.

The results indicate that the total concentration of Cu increased with increases in organic matter. This coincides with the findings of other researchers that Cu has a very high affinity for organic matter (McBride and Blasiak, 1979).

Table 2: The concentrations of water-soluble metals in the soil extract solution (1:2).

Element	5-10 cm	10-15 cm	15-20 cm
		mg L^{-1}	
Al	0.05	2.26	0.128
B	0.012	0.014	0.003
Ba	0.032	0.042	0.028
Ca	15	3.07	4.61
Cd	0.037	0.016	0.016
Cr	< D. L.	< D. L.	< D. L.
Cu	0.133	0.043	0.05
Fe	0.117	1.23	0.231
K	7.31	2.81	2.67
Mg	6.22	1.45	2.03
Mn	0.072	0.036	0.037
Mo	< D. L.	0.008	< D. L.
Na	0.828	< D. L.	< D. L.
Ni	< D. L.	< D. L.	< D. L.
P	0.12	0.13	0.05
Pb	0.464	0.052	0.142
Si	< D. L.	< D. L.	< D. L.
Sr	0.052	0.011	0.016
Ti	< D. L.	0.023	< D. L.
V	< D. L.	0.001	< D. L.
Zn	3.25	1.42	1.51

Table 3: Basic physicochemical properties of studied soil samples.

Depth	pH	Sand	Silt	Clay	IC	OM
cm				%		
0--5		46.1	41.0	12.9	0.017	29.7
5--10	6.81	17.6	50.7	31.7	0.425	10.7
10--15	6.96	54.7	32.1	13.2	0.01	2.09
15--20	6.74	29.5	33.2	37.3	< D. L.	4.52

Table 4: Total element concentrations of studied soil samples and the average concentration and common range in soils (0-5; 5-10; 10-15; 15-20 cm) (mg kg^{-1}).

	0-5	5-10	10-15	15-20	Average in soils[1]	Common range[1]	
			cm				
Al	42,500	54,900	54,800	55,900	71,000	10,000	300,000
B	91.1	247	85.1	242	10	2	100
Ba	419	211	766	938	430	100	3,000
Ca	11,100	10,500	5,220	3,840	13,700	7,000	500,000
Cd	107	81.6	37.2	70.5	0.06	0.01	0.7
Cr	27.7	43.3	33	25.7	100	1	1,000
Cu	584	736	65.4	335	30	2	100
Fe	42,100	74,100	25,700	76,300	38,000	7,000	550,000
K	16,100	20,200	27,000	24,400	8,300	400	30,000
Mg	6,410	9,620	5,520	6,610	5,000	600	6,000
Mn	3,060	2,610	555	3,330	600	20	3,000
Mo	9.64	2.52	0.76	< D. L.	2	0.2	5
Na	4,520	3,25	10,900	5,280	6,300	750	7,500
Ni	13.2	12.7	9.8	11.3	40	5	500
P	2,900	2,210	944	1,330	600	200	5,000
Pb	7,838	49,300	409	12,900	10	2	200
Si	194	424	313	376	320,000	230,000	350,000
Sr	125	184	155	129	200	50	1,000
Ti	2,820	3,000	4,640	3,160	4,000	1,000	10,000
V	57.3	100	63.8	109	100	20	500
Zn	12,900	21,200	2,790	11,500	50	10	300

[1] Lindsay, W. L. 1979.

Table 5 shows the concentrations of elements from chemical extractions of soil samples. The concentrations of amorphous relative to crystalline iron oxides were 1.2; 0.43; and 0.58 at depths 5-10, 10-15 and 15-20 cm respectively (Fig. 3). Table 1 shows that soil, from depths of 5-10 cm, has more organic matter and phosphate and less sand. According to Schwertman and Cornell (2000), freshly precipitated ferrihydrite reacts very strongly with organics, phosphate and silicate species. These inhibitors stabilize ferrihydrite and prevent its transformation by further crystallization. The slow decomposition of organic matter may later allow the formation of more crystalline iron oxides but make that transformation slow. Iron oxide minerals (amorphous and crystalline) relative to total iron were around 73 percent at depths of 5-10 cm, whereas they were around 50 percent at other depths.

Table 6, 7 and 8 show the concentrations and percentage of forms of some elements obtained by selective chemical extraction. For each element, the difference between the total concentration and the sum of the selective extractants is the residual fraction. The quantity of each metal in the exchangeable form for Zn, Cu and Pb was not affected by soil texture. The results indicate that after residual, the most common form of Cd of all soil samples was the exchangeable form. Thus, it seems that exchangeable Cd is an important fraction in this contaminated soil. Also, the fraction of Cd which was associated with crystalline iron oxide minerals was greater than that associated with amorphous iron oxide minerals. Moreover, amorphous iron oxides have very high surface area comparing with crystalline iron oxides which suggests that amorphous iron oxides should adsorb more Cd than crystalline iron oxides. Xian (1987) and Hickey and Kittrick (1984) reported that the exchangeable Cd fraction was the highest compared to

Table 5: Results of selective chemical extractions of soil samples collected from three depths.

Element	5-10 cm				5-10 cm				5-10 cm			
	Water	Exch.	A.A.O.D.	C.B.D.	Water	Exch.	A.A.O.D.	C.B.D.	Water	Exch.	A.A.O.D.	C.B.D.
	mg kg^{-1}											
Al	0.1	6.03	1720	1380	4.52	4.5	702	746	0.255	7.13	825	1170
B	0.023	< D. L.	55	69.1	0.029	< D. L.	5.79	8.55	0.005	< D. L.	9.9	64.5
Ba	0.064	2.95	45.7	89.4	0.084	13.9	2.97	119	0.056	12.6	86.2	184
Ca	29.9	668	7.6	1190	6.13	536	48.4	864	9.22	831	10.5	1010
Cd	0.074	20.7	4.38	10.2	0.033	20.6	2.56	4.12	0.033	26.9	1.63	8.03
Cr	< D. L.	< D. L.	< D. L.	< D. L.	< D. L.	< D. L.	< D. L.	< D. L.	< D. L.	< D. L.	< D. L.	< D. L.
Cu	0.266	0.867	367	9.18	0.085	0.092	3.99	0.053	0.101	0.128	71.2	0.293
Fe	0.234	0.67	29600	24600	2.46	0.078	3840	9040	0.462	0.156	14100	24200
K	14.6	35.1	4.54	830	5.61	53.9	< D. L.	629	5.34	60.4	< D. L.	1090
Mg	12.4	417	2360	652	2.89	70.1	7.6	510	4.05	162	98.5	619
Mn	0.145	4.84	434	276	0.071	5.74	35.2	132	0.073	8.16	484	543
Mo	< D. L.	0.202	5.1	8.24	0.016	0.133	< D. L.	< D. L.	< D. L.	0.157	< D. L.	3.49
Na	1.66	< D. L.	< D. L.	< D. L.	< D. L.	1.02	< D. L.	< D. L.	< D. L.	0.334	< D. L.	< D. L.
Ni	< D. L.	0.033	4.08	0.033	< D. L.	0.015	2.01	< D. L.	< D. L.	0.033	< D. L.	< D. L.
P	0.24	0.791	1030	889	0.26	0.485	164	86.3	0.1	0.548	109	498
Pb	0.927	475	3600	131	0.103	5.64	< D. L.	1.56	0.283	228	1570	42.1
Si	< D. L.	< D. L.	< D. L.	< D. L.	< D. L.	< D. L.	< D. L.	< D. L.	< D. L.	< D. L.	< D. L.	< D. L.
Sr	0.103	3.01	0.118	12.2	0.021	2.45	0.65	6.58	0.032	3.76	0.995	12.9
Ti	< D. L.	< D. L.	7.23	1.34	0.046	< D. L.	4.87	9.87	0.001	< D. L.	1.56	1.97
V	< D. L.	< D. L.	< D. L.	< D. L.	0.002	34600	< D. L.	< D. L.	< D. L.	< D. L.	4.2	< D. L.
Zn	6.5	180	2060	2330	2.83	130	231	1230	3.02	163	1200	1930

Water: Water Soluble; Exch. :$MgCl_2$ (1 M); A.A.O.D.: Acid Ammonium Oxalate in Darkness; C.B.D.: Citrate- bicarbonite-dithionite.

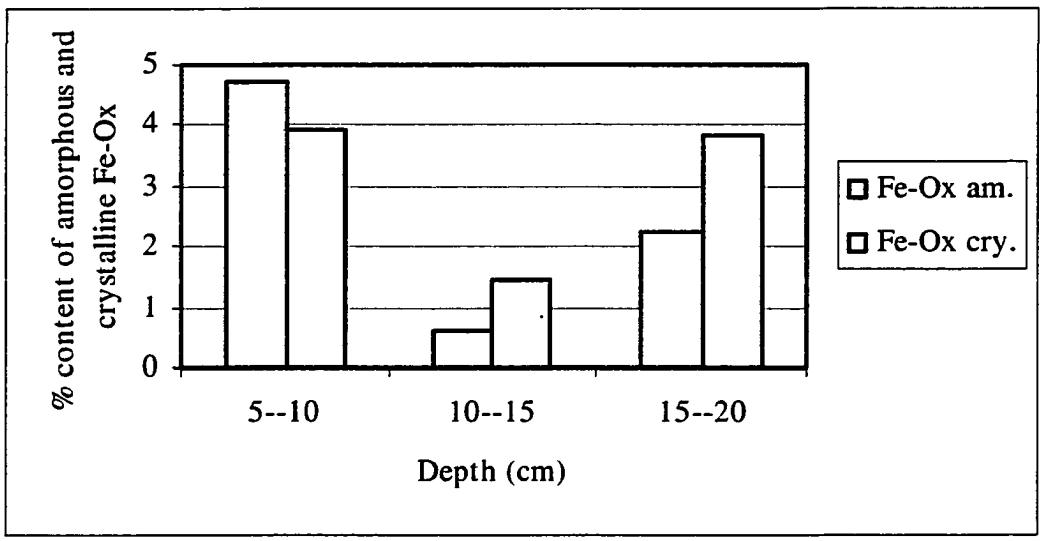

Fig. 3: The percentage content of amorphous and crystalline iron oxides.

Table 6: Concentration and percentage of forms of some elements in the 5-10 cm soil sample.

Element	Water		Exch.		A.A.O.D.		C.B.D.		Total
	mg kg^{-1}	%	mg kg^{-1}	%	mg kg^{-1}	%	mg kg^{-1}	%	mg kg^{-1}
Cd	0.074	0.091	20.7	25.4	4.38	5.36	10.2	12.5	81.6
Cu	0.266	0.036	0.867	0.118	367	49.9	9.18	1.25	736
Fe	0.234	0.0	0.67	0.001	29,600	39.9	24,640	33.2	74,100
Mn	0.145	0.006	4.84	0.186	434	16.7	276	10.6	2,610
Pb	0.927	0.002	475	0.962	3,600	7.3	131	0.265	49,300
Zn	6.5	0.031	180	0.846	2,060	9.7	2,330	11	21,200

Water: Water Soluble; Exch.: $MgCl_2$ (1 M); A.A.O.D.: Acid Ammonium Oxalate in Darkness; C.B.D.: Citrate- bicarbonite- dithionite.

Table 7: Concentration and percentage of forms of some elements in the 10-15 cm soil sample.

Element	Water		Exch.		A.A.O.D.		C.B.D.		Total
	mg kg^{-1}	%	mg kg^{-1}	%	mg kg^{-1}	%	mg kg^{-1}	%	mg kg^{-1}
Cd	0.033	0.089	20.6	55.4	2.56	6.89	4.12	11.1	37.2
Cu	0.085	0.13	0.092	0.141	3.99	6.09	0.053	0.08	65.4
Fe	2.46	0.01	0.078	0.0	3,840	14.9	9,040	35.2	25,700
Mn	0.071	0.013	5.74	1.03	35.2	6.34	132	23.7	555
Pb	0.103	0.025	5.64	1.38	0.0	0.0	1.56	0.381	409
Zn	2.83	0.101	130	4.65	231	8.27	1,220	44	2,790

Water: Water Soluble; Exch.: $MgCl_2$ (1 M); A.A.O.D.: Acid Ammonium Oxalate in Darkness; C.B.D.: Citrate- bicarbonite- dithionite.

Table 8: Concentration and percentage of forms of some elements in the 15-20 cm soil sample.

Element	Water		Exch.		A.A.O.D.		C.B.D.		Total
	mg kg^{-1}	%	mg kg^{-1}	%	mg kg^{-1}	%	mg kg^{-1}	%	mg kg^{-1}
Cd	0.033	0.047	26.9	38.1	1.63	2.31	8.03	11.4	70.5
Cu	0.101	0.03	0.128	0.038	71.2	21.2	0.293	0.087	335
Fe	0.462	0.001	0.156	0.0	1,410	18.4	24,200	31.7	76,300
Mn	0.073	0.002	8.16	0.245	484	14.5	543	16.3	3,330
Pb	0.283	0.002	228	1.76	1,570	12.1	42	0.325	12,900
Zn	3.02	0.026	163	1.42	1,200	10.5	1,930	16.8	11,50

Water: Water Soluble; Exch.: $MgCl_2$ (1 M); A.A.O.D.: Acid Ammonium Oxalate in Darkness; C.B.D.: Citrate- bicarbonite- dithionite.

other fractions of Cd. Cavallaro and McBride (1978) concluded that Cd is likely to be more mobile in soil than Cu. Also, they suggested that ion exchange is responsible for Cd adsorption, but Cu may be bonded more specifically. Kuo et al. (1983) and Song et al. (1999) found the proportion of the exchangeable form of Cd was high. Karlsson et al. (1988) noted that in acid soils, Cd may be associated with the exchangeable and oxide fractions. Moreover, Alloway (1990b) noticed that adsorption processes control the distribution of Cd between the solution and solid phases in contaminated soils rather than precipitation. Therefore, Cd had the most mobility and bioavailability of any metals for that soil. Hickey and Kittrick (1984) reached the same conclusion.

Other than the residual fraction, the most important fraction of Zn in these soil samples was associated with crystalline iron oxide minerals. As Cd, this result is not consistent with the results of modeling and the high surface area of amorphous iron oxides comparing with crystalline iron oxides. Also, Kuo et al. (1983) found that most of the Zn was associated with amorphous iron oxides, and small amounts were extractable by citrate-dithionite-bicarbonate (C.D.B.) solution. The exchangeable fraction was the lowest fraction. Song et al. (1999) found that the proportion of the exchangeable form of Pb was extremely low.

Tables 6, 7 and 8 show that the highest fraction of Cu was associated with amorphous iron oxide minerals for all soil samples. The fraction of exchangeable Cu was the lowest except for the soil sample at a depth of 10-15 cm. Kuo et al. (1983) found that most of the Cu was present in an oxalate-extractable fraction, and small amounts were extractable by a citrate-dithionite-bicarbonate (C.D.B.) solution. They suggested

that Cu was more strongly associated with amorphous iron oxides, with only small amounts being occluded in crystalline iron oxides.

The highest fraction of Pb other than residual was associated with amorphous iron oxides except at depth of 10-15 cm. That may be because of the low amount of amorphous iron oxides at a depth of 10-15 cm. Some researchers noticed that in acid soils, much of the Pb is adsorbed to amorphous Fe oxides (Elliot et al., 1986; Karlsson et al., 1988; and Tessier et al., 1979). The fraction of Pb which is associated with crystalline iron oxides was less than the exchangeable fraction of Pb. Song et al. (1999) and Chlopecka et al. (1996) found that the proportion of the exchangeable form of Pb was extremely low.

In contrast, Levy et al. (1992) found that Pb and Zn were predominantly associated with the Fe and Mn oxides for the same location as our study. They determined metals adsorbed to the surface of Fe and Mn oxides by using 0.25 M NH_2OH-HCl in 25% CH_3COOH. The difference in chemical reagents used in their study vs. our study may explain why we determined that a lower percentage of Pb and Zn are associated with Fe oxides.

The largest amounts of metal in the chemically untreated size fraction tend to be associated with the silt and sand fraction at depths of 15-20 cm; 77.3 percent for Cd; 73.69 percent for Cu; 76.9 percent of Pb; and 69.37 percent for Zn. This could be explained by the fact that the separation of the clay fraction from the sand and silt fractions was done by mechanical dispersion which doesn't provide complete separation of clays. Chlopecka et al. (1996) found that there is little influence of soil texture on the distribution of trace metals between the different extractable forms. In contrast, Ramos et

al. (1994) reported that the distribution of Cu, Pb, Cd and Zn depended on soil texture aside from other soil properties.

SOIL MINERALOGICAL ANALYSES.

The XRD patterns of clay can be seen in figures 4, 5 and 6 and appendices 2-4 show the diffraction data. The mineralogical analysis performed by XRD showed that all of the soil samples have similar minerals. Illite (10.0 Å, 4.99 Å and 3.34 Å) and kaolinite (~7.15 Å and ~ 3.57 Å) were the dominant minerals with minor quartz. Vermiculite might be present in the clay fraction.

From figures 4, 5 and 6, kaolinite was identified by the presence of the 7.14-7.16 Å and 3.57-3.58 Å peaks for the K-saturated treatment and their disappearance after heating at 550 °C. Illite could be identified by the persistence of the 9.93-10.2 Å, 4.96-5.0 Å, 3.33-3.34 Å, and 1.99-2.0 Å peaks for all treatments (K-saturated, K-saturated after 550 °C heating, Mg saturated, and Mg saturated after salvation by GEME).

Peak (001) of illite, which is at 10.0 Å, should have the highest intensity. But, the studied samples had the highest intensity peak at 3.34 Å. Also, that peak is very sharp. So, the presence of quartz in studied samples was suggested (Moore and Reynolds, 1997). This suggestion was supported by the presence of other peaks at 4.24-4.26 Å (100) and 1.81-1.82 Å (112).

Furthermore, all clay fractions produced spacing at14.08-14.45 Å with Mg-saturated treatment . After ethylene glycol monoethyl ether solvation, these samples produced peaks at 16.44-16.61 Å. Mg-vermiculite should have a d (001) of 14.5 Å,

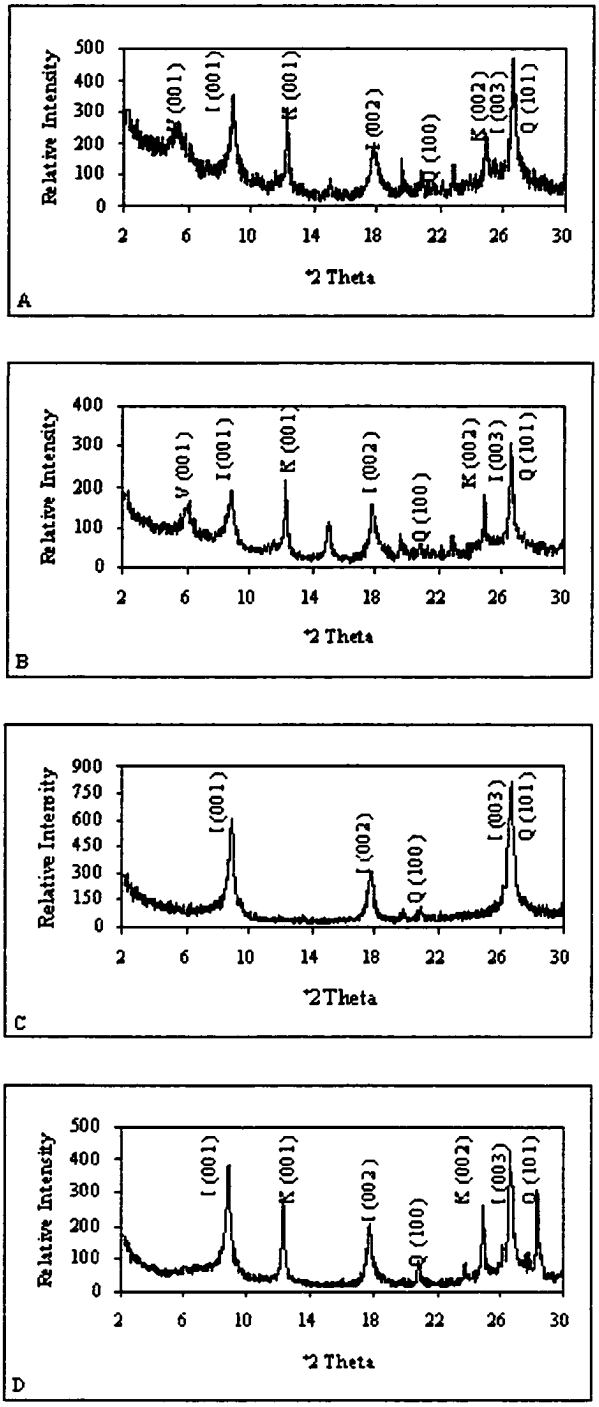

Fig. 4: XRD analysis of clay fraction of the soil sample at a depth of 5-10; (A) Mg-EG; (B) Mg; (C) K 550°C; and (D) K treatment.

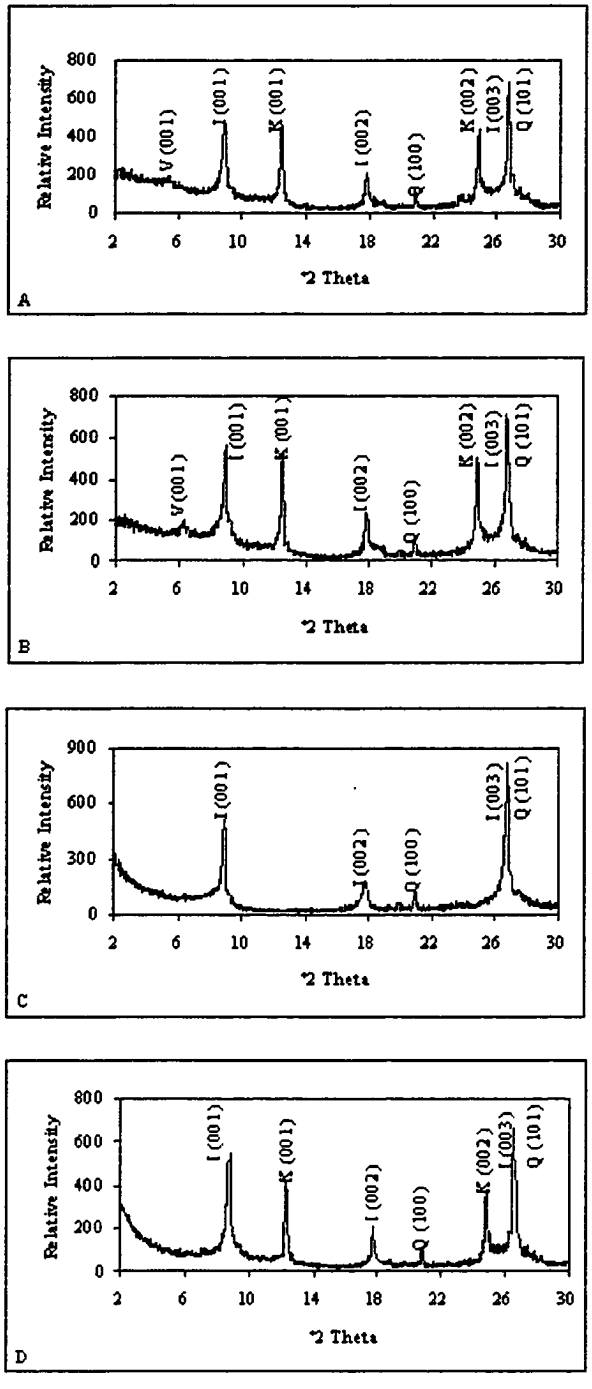

Fig. 5: XRD analysis of clay fraction of the soil sample at a depth of 10-15; (A) Mg-EG; (B) Mg; (C) K 550 C; and (D) K treatment.

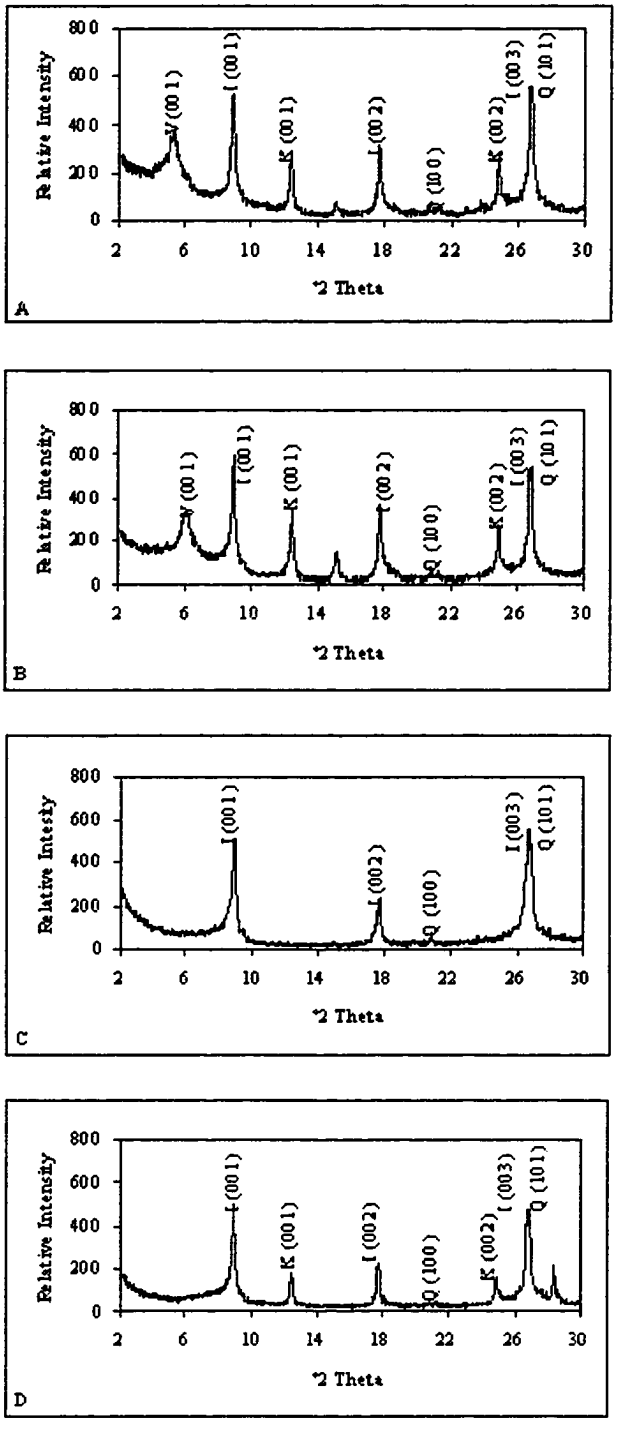

Fig. 6: XRD analysis of clay fraction of the soil sample at a depth of 15-20; (A) Mg-EG; (B) Mg; (C) K 550°C; and (D) K treatment.

which collapses to 10 Å after treatment with k-saturation (Moore and Reynolds, 1997). Therefore, a minor of amount vermiculite might be suggested.

Figures 7, 8 and 9 show the X-ray diffraction patterns of untreated clay, silt and sand fractions of soil samples at 5-10, 10-15 and 15-20 cm and appendices 5-7 show diffraction data. Quartz (3.34 Å, 4.25 Å, etc.) was a major mineral in the sand and silt fractions at all three depths. Therefore, the XRD patterns of soil samples show large differences in mineralogy between the clay, silt and sand fractions.

At depths of 15-20 cm, goethite in the chemically untreated clay fraction can be recognized by its strong peaks (110) and (130) at 4.16 Å and 2.70 Å respectively. Moreover, there is a peak at 2.45 Å, which could be the (111) of goethite and/or the (110) of quartz (Schwertmann and Taylor, 1989). Decreasing the intensity of that peak of silt and sand fractions supported this suggestion. Quartz is generally concentrated in the coarse size fraction whereas goethite is concentrated in fine size fraction.

It is often hard to distinguish amorphous iron oxide minerals by XRD. Because of a low level of crystallinity of these minerals, they are characterized by broad and weak diagnostic XRD reflections. Therefore, more intense XRD peaks from other minerals usually overlap them.

From semi quantitative analysis, illite was found to be the most abundant clay mineral throughout all of depths. The percentage of kaolinite was more than quartz, which was the lowest.

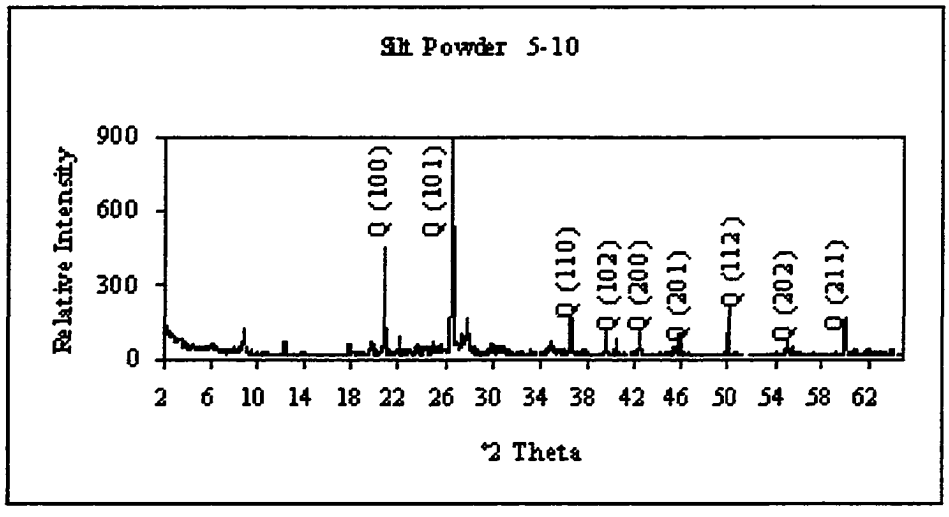

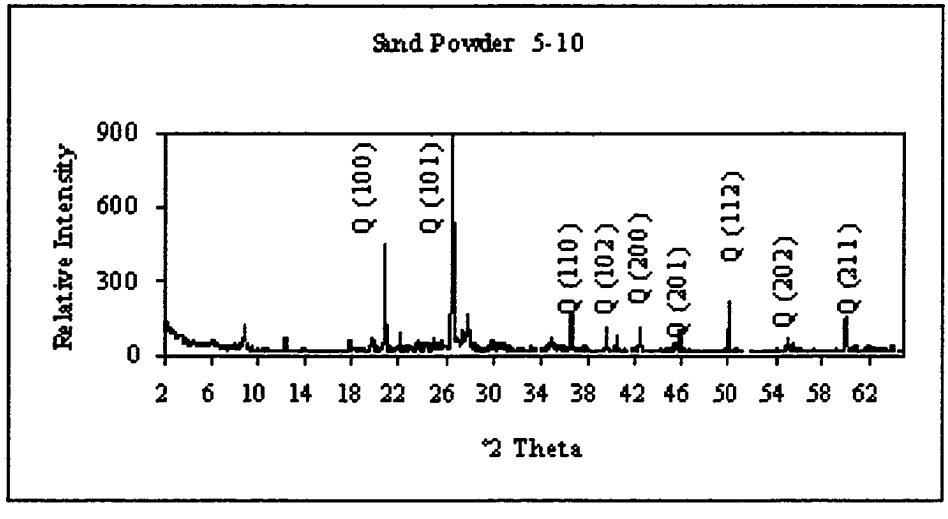

Fig. 7: XR powder diffraction of silt and sand fractions of the soil sample at a depth of 5-10 cm.

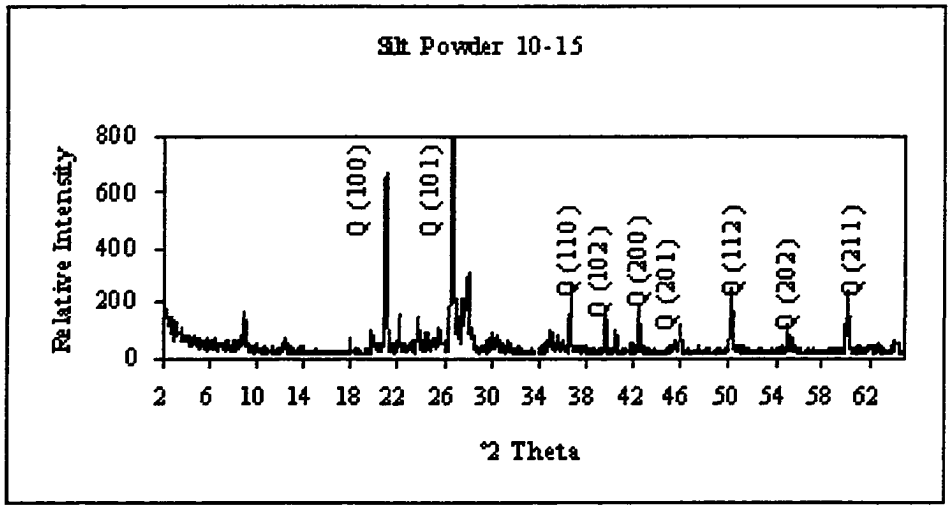

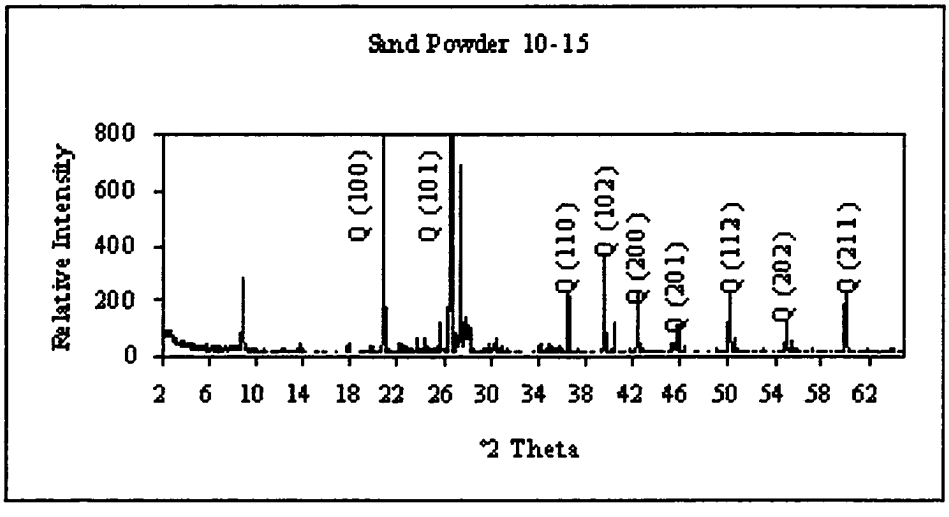

Fig. 8: XR powder diffraction of silt, and sand fractions of the soil sample at a depth of 10-15 cm.

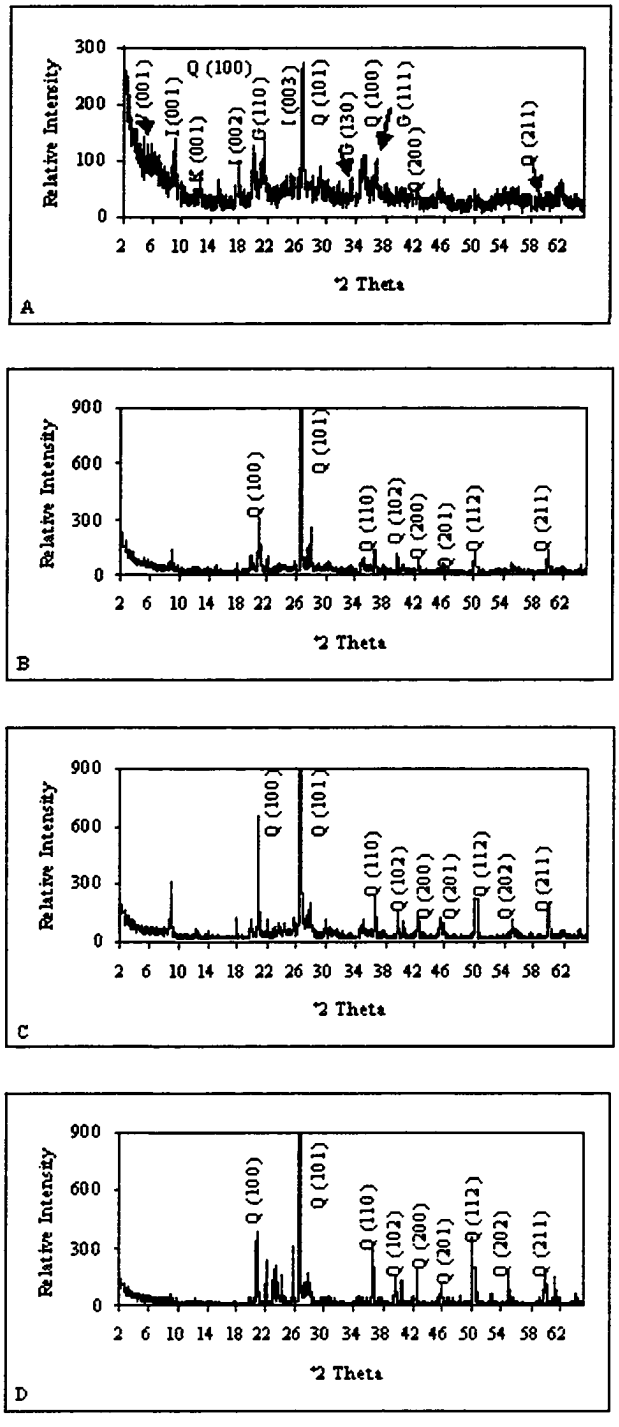

Fig. 9: XR powder diffraction of untreated clay (A); untreated sand and silt (B); silt (C); and sand (D) of the soil sample at a depth of 15-20 cm.

ELECTRON MICROPROBE

Figures 10-13 show the backscattered electron images and X-ray maps for Fe, Pb, Zn, Cu and Cd for particles of the whole soil sample and the chemically untreated clay fraction at a depth of 15-20 cm. For both the whole soil sample and the clay fraction Fe, fraction Fe, Zn, and Pb were abundant.

For the whole soil (Figures 10 and 11), it is clear from the Fe and Pb dot maps that there is a visible association between Fe and Pb. This is apparent by the gray areas on the Fe dot map that were spatially associated with the gray areas on the Pb dot map. There are some areas of Pb and Fe enrichment which occur separately, as determined by comparing the exact positions of Pb and Fe particles using grids. These spots are labeled in the figures. Moreover, figure 9 shows a coating of secondary iron oxides around an iron-free particle. The strong association between Pb and Fe is especially apparent in this coating.

In contrast, the gray areas on the Zn dot map were not associated with these locations on the Fe dot map, particularly in figure 11. A prime example of the lack of association between Zn and Fe is illustrated by comparing the gray region in the lower right hand corner with the same location on the Fe dot map, which displays a dark Fe void. The dot map of Zn in figure 10 shows that distribution of Zn extended to more areas compared with Fe or Pb.

As above, the chemically untreated clay fraction showed the same trend as for the whole soil. Figure 12 shows an area with an association of Fe and Pb (identified by 2 arrows). Furthermore, the dot map of Zn illustrates that the occurrence of Zn does not

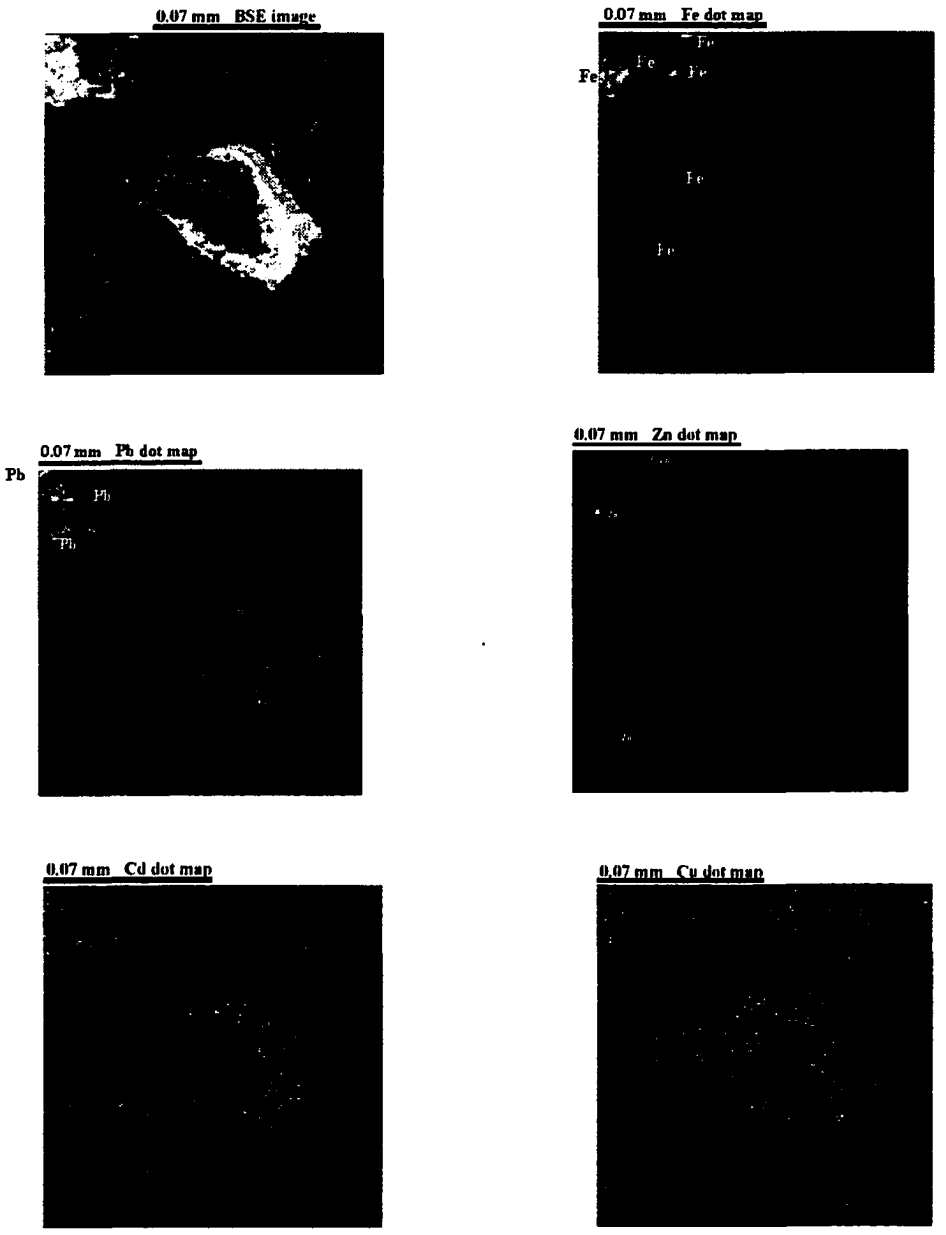

Fig 10: Backscattered electron image, and dot maps of Fe, Pb, Zn, Cd and Cu; of soil (≤ 2 mm).

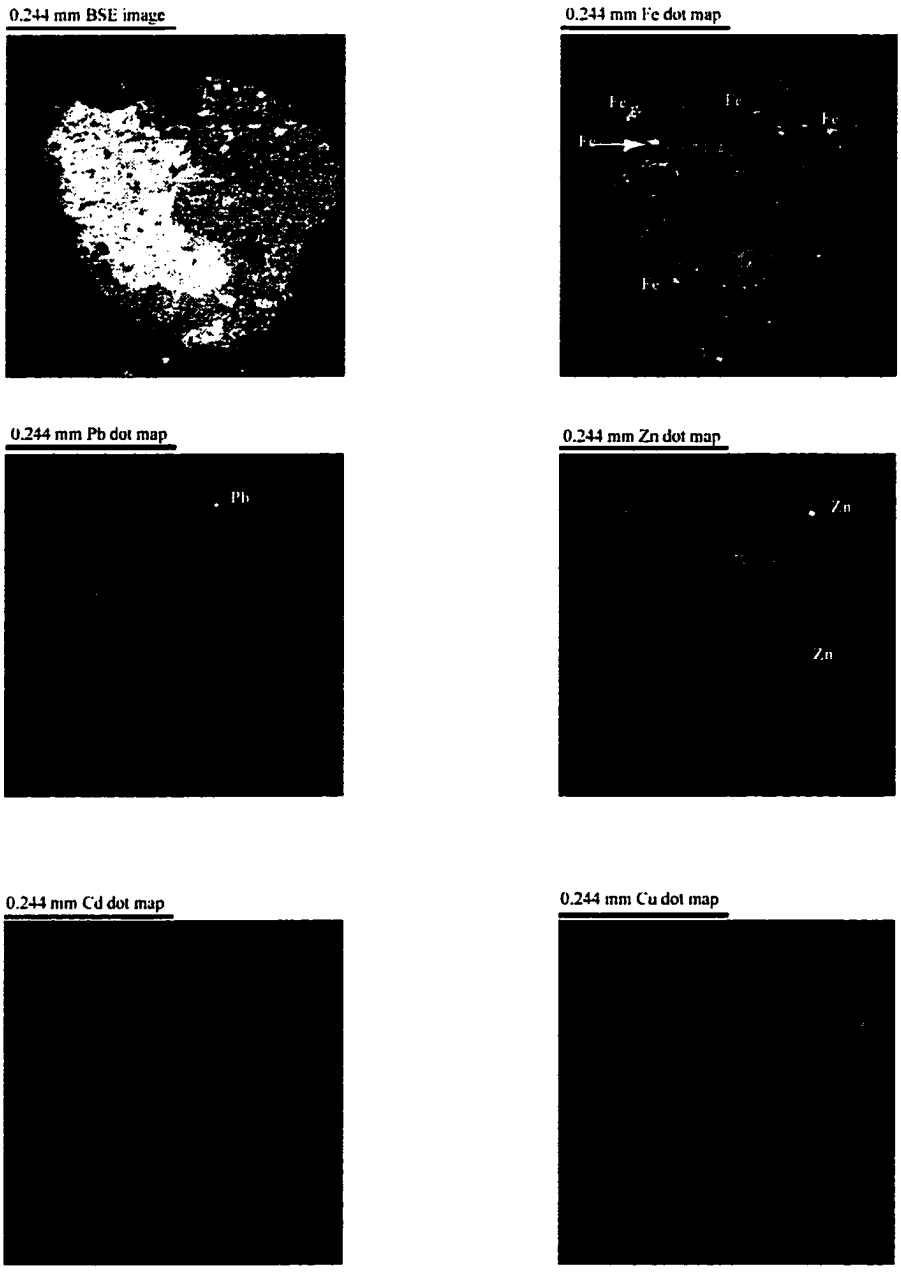

Fig 11: Backscattered electron image, and dot maps of Fe, Pb, Zn, Cd and Cu; of soil (≤ 2 mm).

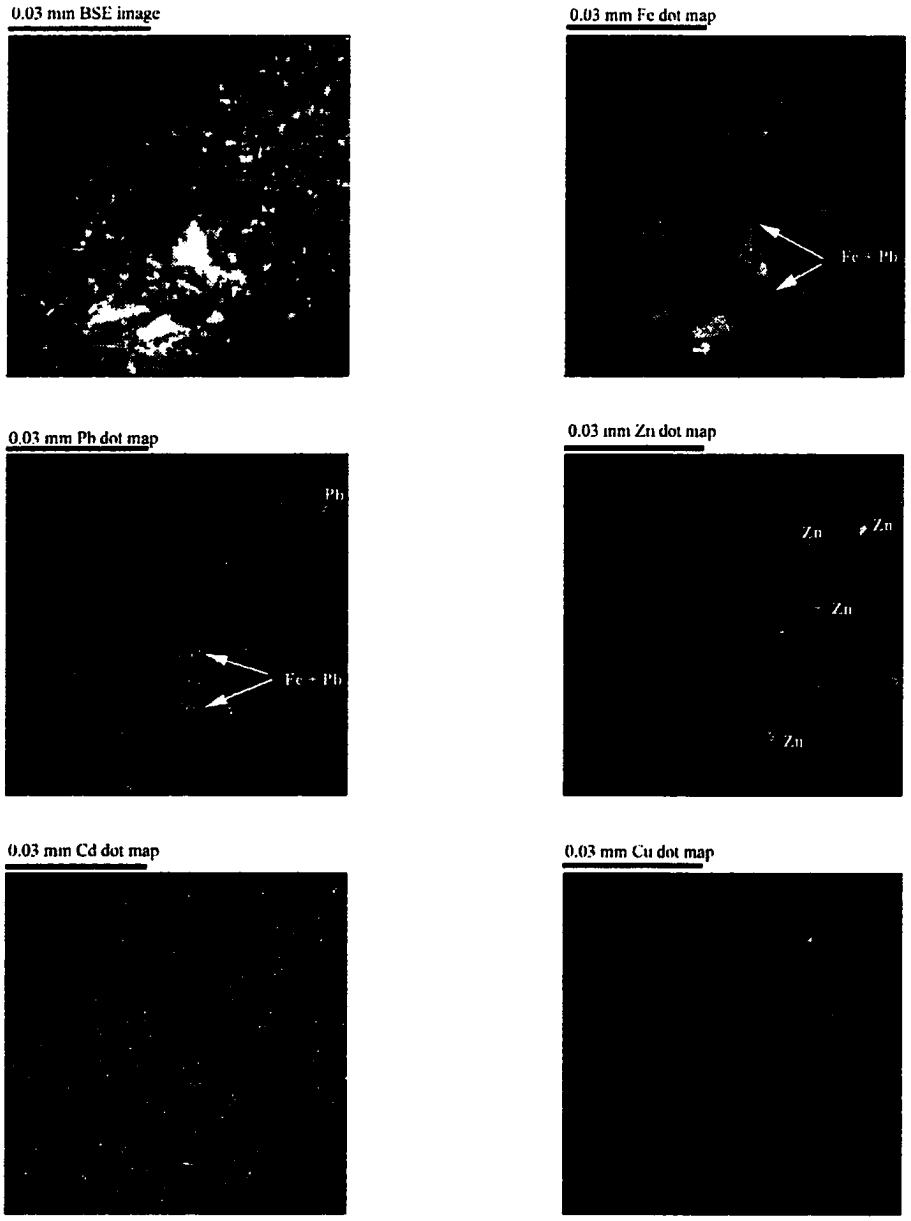

Fig 12: Backscattered electron image, and dot maps of Fe, Pb, Zn, Cd and Cu; of clay fraction (untreated chemically).

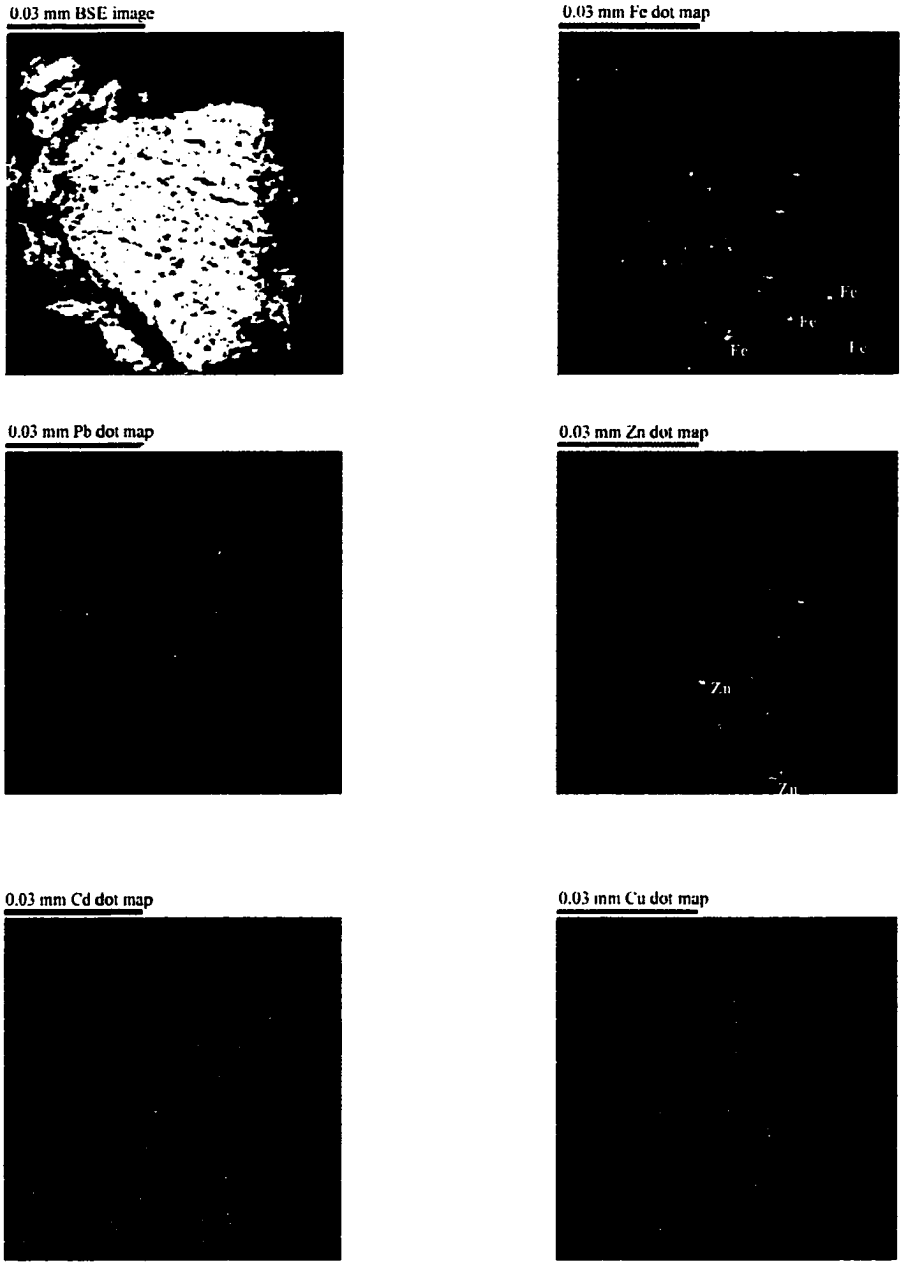

Fig 13: Backscattered electron image, and dot maps of Fe, Pb, Zn, Cd and Cu; of clay fraction (untreated chemically).

match the distribution of Fe. Moreover, there were some isolated particles rich in Pb or Zn which were not associated with Fe.

From above, the association of Pb with Fe is more pronounced than is Zn with Fe. Brummer (1986) mentioned that Pb is more strongly adsorbed to iron oxides compared to Zn (Alloway, 1990). This is also consistent with the greater values for adsorption constants for Pb vs. Zn. Other researchers have reported that a high proportion of Pb was associated with the oxide fraction (Sposito et al., 1982; Chlopecka, 1993; Ramos et al., 1994; and Yarlagadda et al., 1995).

Cavallaro and McBride (1984) found that crystalline oxides appear to have a significant role in Zn adsorption. Shuman (1988) found that Fe oxides are important in Zn adsorption. Moore et al. (1988) and Karlsson et al. (1988) noticed that Zn might exist mainly in the oxide fraction in acid soils. Kuo et al. (1983) found that most of the Zn was associated with amorphous iron oxides and small amounts were extractable by citrate-dithionite-bicarbonate (C.D.B.) solution. However, our results from electron microprobe indicate only a minimal association between Fe and Zn.

TRANSMISSION ELECTRON MICROSCOPE ANALYSIS

Identification of Iron Oxide Minerals

Goethite crystals commonly appear under the electron microscope as acicular and elongated along the crystallographic direction. The typical size of synthetic goethite crystals usually is around > 200 nm. In soil, the acicular shape may exist but often is less well expressed. Also, they generally exhibit a needle length of 50-100 nm, but sub-rounded or mono-dimensional crystals may be less than 20 nm in cross section. In

contrast, ferrihydrite forms very small spherical particles, 3-7 nm in diameter (Schwertmann and Taylor, 1989 and Schwertmann and Cornell, 2000).

TEM micrographs and microbeam ED patterns from iron oxide minerals in the soil sample are shown in figures 14-18. The length of crystals ranges from around 225 nm to 525 nm, and the width ranges from 70 nm to 225 nm. This is the general size of secondary iron oxide minerals (Schwertmann and Cornell, 2000). Also, figure 14 shows spherical particles which are aggregated with a diameter of 150 nm. These particles are comparable to previously identified amorphous iron oxide minerals and do not produce an ED pattern. Figure 15 illustrates a crystalline Fe-oxide mineral particle and its ED pattern which is typical of a single crystal. Other particles produced ED patterns which are typical of multiple crystals, with multiple offset patterns. Figures 16-18 indicate that these soil particles exhibit both crystalline and amorphous characteristics and may consist of a combination of these.

Synthetic Goethite

Figures 19-21 show TEM micrographs and microbeam ED patterns for some particles of synthetic goethite. These particles are very similar to Fig. 15, although greater in size.

Quantitative Analysis of Pb Concentration in Soil Particles

Table 9 shows the Pb concentrations from TEM/EDX of five soil Fe-oxide particles. The average Pb concentration was 42900 on the basis of mg Pb per kg of Fe oxide. As we explained above, amorphous iron oxides have high surface area so it is predicted to have more concentration of Pb than goethite as the results of modeling and

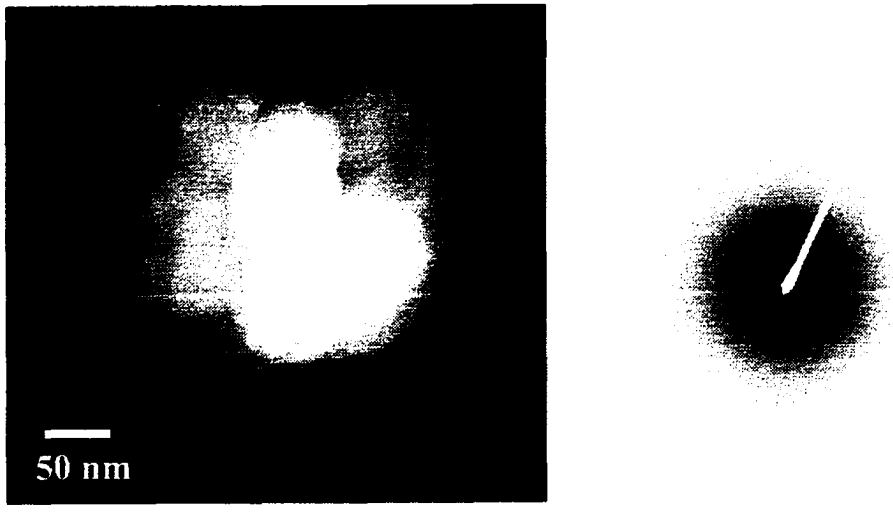

Fig. 14: TEM micrograph and microbeam ED patterns of soil sample (particle 1).

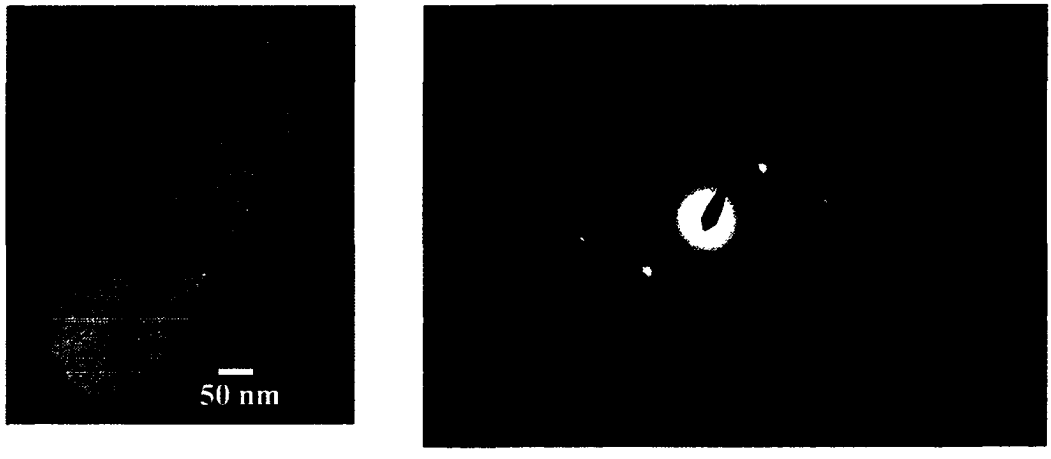

Fig. 15: TEM micrograph and microbeam ED patterns of soil sample (particle 2).

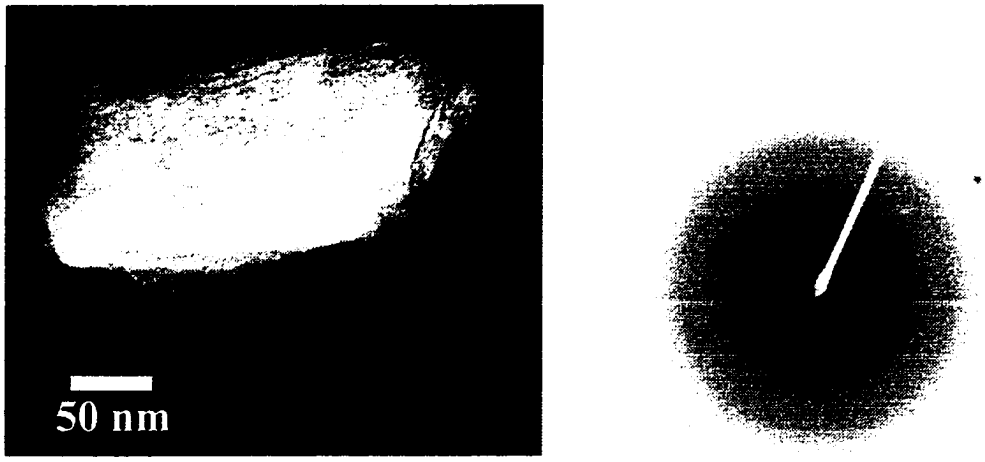

Fig. 16: TEM micrograph and microbeam ED patterns of soil sample (particle 3).

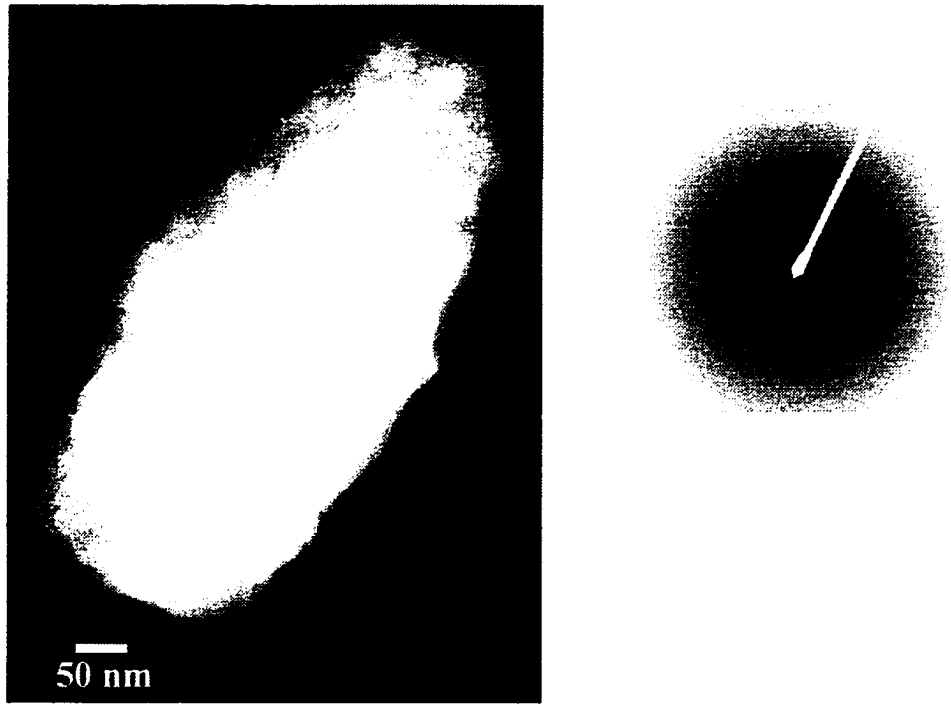

Fig. 17: TEM micrograph and microbeam ED patterns of soil sample (particle 4).

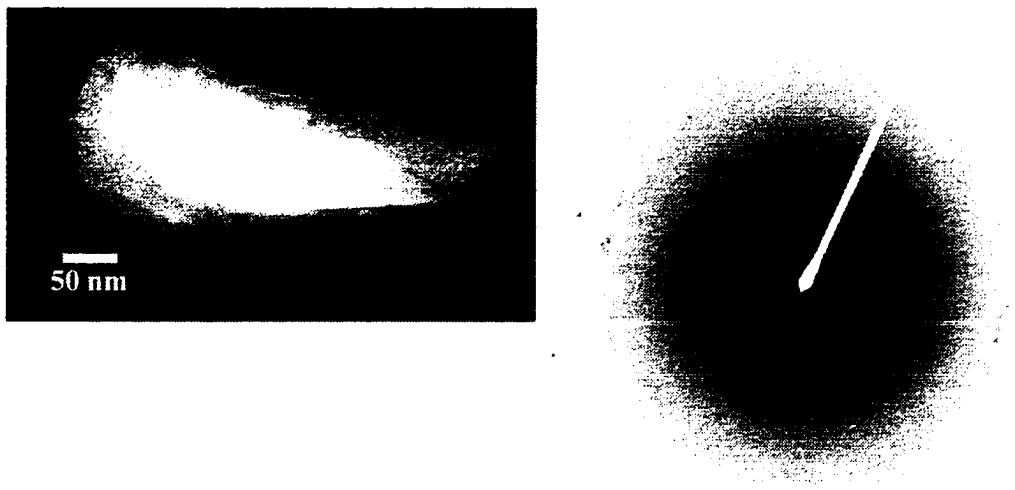

Fig. 18: TEM micrograph and microbeam ED patterns of soil sample (particle 5).

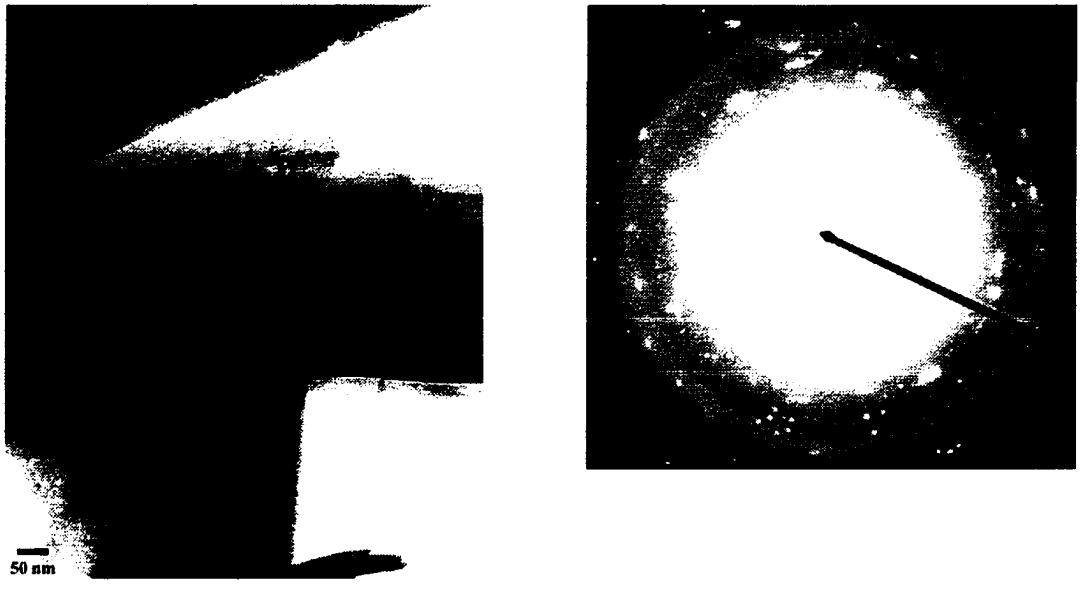

Fig. 19: TEM micrograph and microbeam ED patterns of synthetic goethite sample.

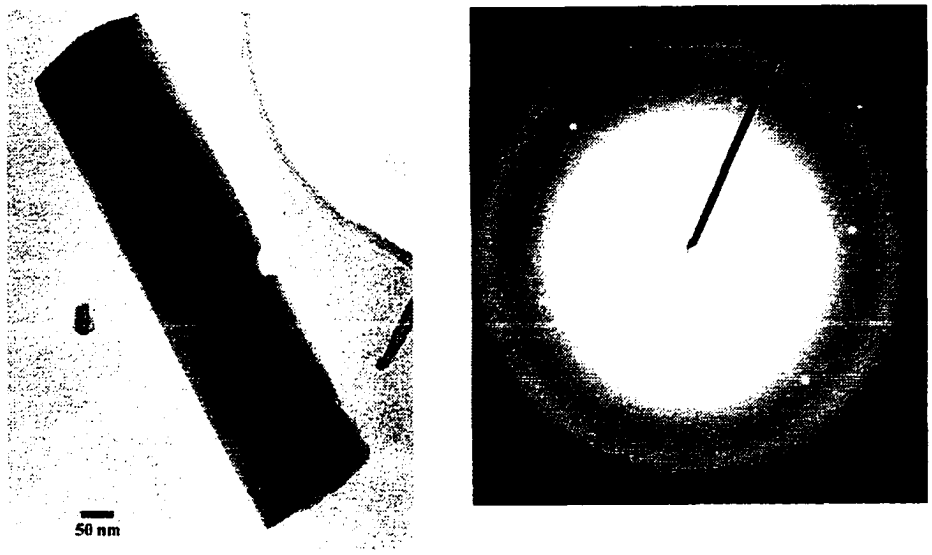

Fig. 20: TEM micrograph and microbeam ED patterns of synthetic goethite sample.

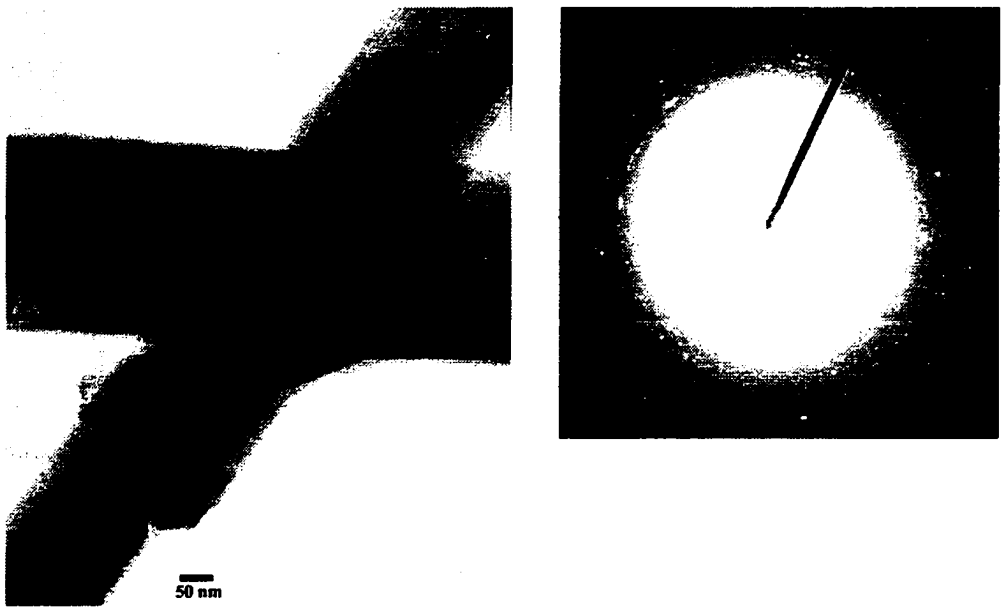

Fig. 21: TEM micrograph and microbeam ED patterns of synthetic goethite sample.

Table 9: The quantitative analysis of five selected particles of the chemically untreated clay sample (15-20 cm).

Particle	Pb mg kg^{-1} Fe-oxide
Particle 1	38,500
Particle 2	40,700
Particle 3	45,700
Particle 4	33,200
Particle 5	56,200
Average	42,900

selective extractions indicated. However, no difference was found in comparing the Pb concentrations in amorphous and crystalline Fe-oxides. The explanation for that would be noticed below.

THE RESULTS OF MODELING WITH MINTEQA2

The percentages of the amorphous and crystalline iron oxide minerals from selective extraction are 4.71 and 3.92; 0.61 and 1.44; and 2.24 and 3.85 for depths at 5-10, 10-15 and 15-20 cm, respectively. As expected, the concentrations of each of these metals were predicted to be much greater in amorphous than for crystalline Fe oxide. The modeled concentrations of Cd, Cu, Pb, and Zn adsorbed to amorphous Fe oxide was approximately 5 to 10 times greater than the concentration of these metals adsorbed to crystalline Fe oxide in many cases. This is consistent with the difference in the values for site density used in modeling, which is very close to 10 times greater for the amorphous than the crystalline Fe oxide.

Comparison of the Results of Sequential Extraction, TEM/EDX and Modeling with MINTEQA2

Tables 10 and 11 show the comparison between the concentrations of heavy metals predicted by MINTEQA2 and the selective extraction. According to the results of MINTEQA2, the sequence of the adsorption of heavy metals to amorphous or crystalline (goethite) iron oxide minerals is Pb> Cu> Zn> Cd. This order of metal affinities for iron oxide minerals (Amorphous and goethite) is in agreement with the results of Kinniburgh et al. (1976) and Schwertmann and Taylor (1989).

Table 10: Metal concentrations adsorbed to the amorphous Fe-oxide minerals as predicted by the DLM vs. the concentrations from selective extraction (Acid Ammonium oxalate in darkness):

Element	5-10 cm			10-15 cm			15-20 cm		
	A.A.O.D*.			A.A.O.D.			A.A.O.D.		
	Minteqa2	Extracted	(Ex./Mi)	Minteqa2	Extracted	(Ex./Mi)	Minteqa2	Extracted	(Ex./Mi)
	mg kg^{-1}(Fe-Oxide**)			mg kg^{-1}(Fe-Oxide**)			mg kg^{-1}(Fe-Oxide**)		
Cd	2.41	93	38.6	3.6	419	117	2.03	72.6	35.7
Cu	26,800	7,800	0.29	27,900	652	0.02	19,200	3,182	0.17
Pb	58,200	76,500	1.31	27,900	< D. L.	0.0	38,100	70,000	1.83
Zn	1,700	43,700	25.8	2,430	37,800	15.5	1,490	53,800	36.2

* A.A.O.D.: Acid Ammonium oxalate in darkness.

** The concentration of heavy metals in the amorphous form of iron oxide minerals.

Table 11: Metal concentrations adsorbed to the crystalline Fe-oxide minerals (goethite) as predicted by the TLM vs. the concentrations from selective extraction (Citrate bicarbonate dithionite):

Element	5-10 cm			10-15 cm			15-20 cm		
	C.B.D.*			C.B.D.			C.B.D.		
	Minteqa2	Extracted	Ex./Mi	Minteqa2	Extracted	Ex./Mi	Minteqa2	Extracted	Ex./Mi
	mg kg^{-1}(Fe-Oxide**)			mg kg^{-1}(Fe-Oxide**)			mg kg^{-1}(Fe-Oxide**)		
Cd	0.0	259		0.0	286		0.0	208	
Cu	53	234	4.41	57.7	3.65	0.06	25.5	7.6	0.3
Pb	6,420	3,340	0.52	6,980	108	0.02	7,140	1,090	0.15
Zn	12.5	5,950	4,764	13.6	85,300	6,280	5.40	50,140	9,290

* C.B.D.: Citrate bicarbonate dithionite.

** The concentration of heavy metals in the crystal form of iron oxide minerals.

The concentration of Pb from selective extraction of amorphous iron oxide minerals was greater than that predicted by the model except at a depth of 10-15 cm (Table 10). The low concentration of Pb in the amorphous Fe-oxide fraction may be because the lowest Pb content is at a depth of 10-15 cm. In contrast, selective extraction of the crystalline iron oxides yielded concentrations of Pb associated with Fe-oxide which were less than predicted by MINTEQA2 at all depths. The low concentration of Pb in the crystalline Fe-oxide fraction could be the result of desorption of adsorbed Pb from the surface of Fe-oxide minerals due to the low pH of the A.A.O.D. reagent. At pH of approximately 3.0, adsorption of Pb to Fe-oxides is minimal (McKenzie, 1980). This could also explain the Pb concentrations from selective extractions, which were greater than model predictions for the amorphous Fe-oxides.

If we subtract the modeled concentration of Pb adsorbed to crystalline Fe oxide from the total concentration of Pb extracted by the A.A.O.D. reagent, we calculate a Pb concentration associated with Fe oxides of 59600 mg kg^{-1}. This value is more similar to the model prediction for adsorption of Pb to amorphous Fe oxides of 38,100 mg kg^{-1}. Dissolution of Pb particles not associated with Fe, as observed by EMP, may also contribute to an overestimation of Pb in the amorphous Fe-oxide fraction.

The low concentration of Pb extracted by the C.B.D. reagent indicates that substitution of Pb in crystalline Fe oxides is of minor importance compared to other mechanisms, as Pb substituted in the crystal structure should not be released by the A.A.O.D. reagent, and should be released following complete dissolution of the Fe oxide particles by C.B.D.

The models predicted that Pb concentration associated with the amorphous Fe oxides should be approximately 5 times greater than the concentration associated with crystalline Fe oxides. The Pb concentrations measured by TEM/EDX revealed very similar concentrations for Pb in amorphous and crystalline Fe oxides. Furthermore, many particles appeared to consist of aggregates including multiple particles of both amorphous and crystalline Fe oxides, which did not allow the differentiation of Pb concentrations associated with these two Fe mineral types.

The unexpected similarity between the adsorption properties of amorphous and crystalline Fe oxides in the soil sample may be the result of differences which exist in the surface chemical properties of soil vs. synthetic crystalline Fe oxides. The particle size of soil goethite particles is often less than synthetic goethite, which would lead to increased surface area, site density, and metal adsorption capacities in the soil Fe oxides. The crystalline soil Fe oxide particle exhibited an irregular surface morphology with the presence of steps and layers, which may also lead to greater surface area compared to synthetic goethite which exhibit a smooth surface. The multiple particle ED patterns produced from several of the soil Fe oxide particles indicates that several small goethite particles may be present (in addition to amorphous Fe-oxide in some cases) in the observed particles. Consequently, the particle size of the soil goethite may be even less than the observed Fe-rich particle dimensions. The particle size of our crystalline soil Fe oxides could be considerably less than synthetic goethite.

The average Pb concentration for all five soil Fe oxide particles analyzed by TEM/EDX was 42,900 mg kg^{-1}. This value is intermediate between the Pb concentration measured for the amorphous fraction of 70,000 mg kg^{-1} from selective extraction and the

model predicted Pb concentration of 38,100 mg kg^{-1} for the amorphous fraction. Since no differences in Pb concentration between amorphous and crystalline Fe oxides were evident by TEM/EDX analysis, it is informative to combine the results from the amorphous and crystalline fractions from selective extraction and also modeling to represent the total Fe oxide content in the soil. The total concentration of Pb associated with amorphous plus crystalline Fe oxides is 26400 mg kg^{-1} from selective extraction, and 18500 mg kg^{-1} from modeling. These values are both less than the Pb concentrations measured for soil particles by TEM/EDX. However, the soil particles analyzed by TEM/EDX may not be representative of all Fe oxide particles in the soil. We separated the colloidal Fe oxide particles from the soil sample by mechanical dispersion (in order to avoid any chemical redistribution of metals), which does not provide complete separation of secondary iron oxides. The average Pb concentration associated with any Fe oxides not separated by the mechanical dispersion process was not determined by TEM/EDX and may be different than for the particles which were analyzed.

Another source of uncertainty in our modeling results is that we assumed the average surface area of our soil Fe-oxide particles was equal to values measured in previous studies. However, the relative affinity of the Fe oxide particles for metals should not depend on surface area. Although limitations exist for the modeling and experimental techniques which we applied, it appears from our results that surface adsorption accounts for most of the Pb associated with Fe oxides. All four of the methods used; selective extraction, EMP, TEM/EDX, and modeling indicated a strong association of Pb with the soil Fe oxides.

The selective extraction results of both amorphous and crystalline iron oxide minerals, for Cd and Zn, were considerably greater than that predicted by the model. Although we do not have quantitative data for Zn from TEM/EDX, EMP indicated a much greater association between Pb and Fe than for Zn and Fe. This is not consistent with the results of selective extraction, which indicated very similar concentrations of Zn and Pb in the amorphous Fe oxide fraction and a much greater concentration of Zn than Pb in the crystalline Fe oxide fraction. The results of EMP analysis are consistent with the modeling, which predicted that the concentration of Zn adsorbed to Fe oxides was much less than for Pb. EMP analysis also indicates that a substantial fraction of the Zn in the soil is present as Zn rich particles which are not associated with Fe oxides. It appears that the Zn-rich particles identified by EMP which are not associated with Fe oxides may be partially dissolved by the A.A.O.D. and C.B.D. reagents, resulting in an overestimation of the Zn concentration in these fractions by the selective extraction method.

For Cu, the selective extraction of both amorphous and crystalline iron oxide minerals was less than the model predictions, except for crystalline Fe oxides at depth 5-10 cm. The concentration of free Cu ions may be less than the total concentration of Cu in the water extracts due to complexation with dissolved organic matter, which could explain the high concentrations of Cu adsorbed by the Fe-oxides that were predicted by the model for amorphous Fe-oxides.

The concentrations of metals associated with Fe oxides predicted by modeling assume that surface adsorption is the dominant mechanism. It is possible that surface precipitation could also contribute to the total retention of metals by Fe oxides. For

example, the high concentrations of both Pb and Zn associated with Fe oxides measured by selective extraction as compared to modeling may be partially due to surface precipitation. Stumm and Morgan (1996) mentioned that at high concentration, adsorption may lead to the formation of a surface precipitate. As mentioned above in the literature review, interactions between hydrous oxides and metals can include adsorption, surface precipitation and substitution. The relative concentrations of sorbate and sorbent decide the dominant mechanism. According to Dzombak and Morel (1990), surface precipitation will occur only when at least 50% of the adsorption sites are occupied by a metal. The soluble metal concentrations present in our samples do not appear to be high enough to cause surface precipitation, as the modeled adsorbed metal concentrations are less than 50% of the adsorption capacity (Table 12). Distinguishing between these processes directly is difficult and requires micro scale analytical methods (Xu et al., 1994).

Table 12: Adsorption capacity of Pb (A) and Zn (B) by amorphous and crystalline iron oxide minerals.

Iron oxide mineral	Site density		Pb adsorption capacity
		mole/g (Fe-Ox)	mg kg^{-1}
Amorphous	Strong Sites	5.63E-5	1.17E+4
	Weak Sites	2.25E-3	4.66E+5
	Total		4.78E+5
Crystalline	Surface area		
	51.8 m^2 g^{-1}*	2.20E-4	4.56E+4
	20 m^2 g^{-1}**	8.49E-5	1.76E+4

Iron oxide mineral	Site density		Pb adsorption capacity
		mole/g (Fe-Ox)	mg kg^{-1}
Amorphous	Strong Sites	5.63E-5	3.68E+3
	Weak Sites	2.25E-3	1.47E+5
	Total		1.51E+5
Crystalline	Surface area		
	51.8 m^2 g^{-1}*	2.20E-4	1.44E+4
	20 m^2 g^{-1}**	2.60E+4	5.55E+3

* : value for goethite surface area from Balistrieri and Murray 1981.

** : value for goethite surface area from Schwertmann and Cornell 2000.

SUMMARY AND CONCLUSIONS

A contaminated soil near Leadville, CO was studied to investigate the behavior of heavy metals (Pb, Zn, Cu and Cd) with iron oxide minerals. The total concentrations of these metals were higher than the common ranges in soils except for the concentration of Cu at depth 10-15 cm.

Forms of iron oxide minerals were determined by using selective extraction solutions A.A.O.D. and C.B.D.. Amorphous and crystalline iron oxide minerals were present at 0.61-4.7 % and 1.4-3.9 % of the total soil mass respectively. Analysis of XRD showed the presence of goethite (crystalline ion oxide) in the clay fraction of the soil sample at a depth of 15-20 cm.

The whole soil sample and the chemically untreated clay fraction at a depth of 15-20 cm were analyzed by using EMP to study the distribution of heavy metals with iron oxides. We found a high proportion of Pb was associated with iron oxides, while Zn was only slightly associated with iron oxides. Moreover, there are some isolated particles of Pb and Zn. Therefore, precipitation of oxide and carbonate forms of these metals should be suggested. It is also possible that these metal-rich particles could be sulfide or sulfate minerals.

The chemically untreated clay fraction of the soil sample at depth 15-20 cm was investigated by TEM with ED and EDX. Five selected particles were analyzed by EDX. An ED pattern was used to identify the presence of crystalline particles. Both amorphous

and crystalline iron oxide particles were observed. The concentration of Pb in these particles ranges from 33,200 to 56,200 mg kg^{-1} of Fe-oxides, and the average was 42,900 mg kg^{-1} of Fe-oxides. The concentration of Pb was similar for crystalline and amorphous particles.

Adsorption of heavy metals (Pb, Zn, Cd and Cu) by amorphous iron oxide and goethite in the soil samples was modeled by using the DLM and TLM respectively. The relative concentrations of heavy metals adsorbed to amorphous iron oxide or goethite is Pb > Cu > Zn > Cd according to the models. The much greater concentration of Pb vs. Zn adsorbed to the Fe-oxide surface is consistent with EMP results.

From the results of modeling, amorphous iron oxide minerals should contain higher concentrations of heavy metals (Pb, Zn, Cd, and Cu) than crystalline iron oxide minerals. The failure to observe this in the soil Fe-oxide particles may be due to differences in the properties of synthetic vs. soil crystalline Fe oxides.

From our results, selective extraction of iron oxides provides a fairly accurate representation of association of Pb with Fe oxides, but not Zn. We do not expect that selective extraction will accurately distinguish the metal concentrations in amorphous vs. crystalline Fe-oxides, since the very low pH of A.A.O.D. results in desorption of all adsorbed heavy metals from the surfaces of all iron oxides (amorphous and crystalline). Also, the low of pH of both the A.A.O.D. and C.B.D. reagents can dissolve oxide, hydroxide and carbonate forms of heavy metals which may be present.

Furthermore, we can conclude that the most important mechanism of interaction of Pb with iron oxides is surface adsorption. The greatest impact on the soluble

concentration of heavy metals might be precipitation rather than adsorption because of the very high concentrations of heavy metals in the soil samples. For the conditions of our study, Pb has the highest association with iron oxide minerals. Therefore, factors which affect iron oxides will affect solubility of heavy metals. For a complete description of the partitioning and solubility of metals in these soils, interactions between the metals and other soils colloids including clays and organic matter must also be considered. Also, precipitation of heavy metals such as carbonates, oxides and hydroxides must be more completely characterized.

REFRENCES

Ahnstrom, Z. S. and Parker, D. R. 1999. Development and Assessment of a Sequential Extraction Procedure for the Fractionation of Soil Cadmium. Soil Sci. Soc. Am. J. 63: 1650-1658.

Allison, J. D.; Brown, D. S.; and Novo-Gradac, K. J. 1991. MINTEQA2/PRODEFA2, a Geochemical Assessment Model for Environmental Systems: Version 3.0 User's Manual. Environmental Research Laboratory Office of Research and Development. U. S. Environmental Protection Agency. Athens, Georgia. Pp. 109.

Alloway, B. 1990a. Introduction. In Heavy Metals in Soils. Edited by B. J. Alloway. John Wiley and Sons, Inc. New York. Pp. 3-6.

Alloway, B. J. 1990b. Cadmium. In Heavy Metals in Soils. Edited by B. J. Alloway. John Wiley and Sons, Inc. New York. Pp. 100-124.

Alloway, B.J. 1990. Soil Processes and Behavior of Metals. In Heavy Metals in Soils. Edited by B. J. Alloway. John Wiley and Sons, New York. Pp. 7–27.

Baker, B. J. 1990. Copper. In Heavy Metals in Soils. Edited by B. J. Alloway. John Wiley and Sons, Inc. New York. Pp. 151-176.

Balistrieri, L. S. and Murray, J. W. 1979. The Surface Chemistry of Goethite (α-FeOOH) in Seawater. In Chemical Modeling in Aqueous Systems, Edited by Jenne, E. A. ACS Symposium Series. No. 93. American Chemical Society, Washington, D.C. Pp. 275-298.

Balistrieri, L. S. and Murray, J. W. 1981. The Surface Chemistry of Goethite (α-FeOOH) in Seawater. Am. J. Sci. 281: 788-806.

Balistrieri, L. S. and Murray, J. W. 1982. The Adsorption of Cu, Pb, Zn and Cd on Goethite from Major Ion Seawater. Geochim. Cosmochim. Acta. 46: 1253-1265.

Bradbury, Michael M. and Baeyens, Bart. 1999. Modeling the Sorption of Zn and Ni on Ca-montmorillonite. Geochim. Cosmochim. Acta. 63 (3-4): 325-336.

Brennan, E. W. and Lindsay, W. L. 1996. The Role of Pyrite in Controlling Metal Ion Activities in Highly Reduced Soils. Geochim. Cosmochim. Acta. 60 (19): 3609-3618.

Brummer, G., Tiller, K. G., Herms, U. and Clayton, P. M. 1983. Adsorption, Desorption and/or Precipitation-Dissolution Processes of Zinc in Soils. Geoderma, 31: 337-354.

Cavallaro, N., and McBride, M. B. 1984. Zinc and Copper Sorption and Fixation by an Acid Soil Clay: Effect of Selective Dissolution. Soil Sci. Soc. Am. J. 48: 1050-1054.

Cavallaro, N., and McBride, M. B. 1978. Cooper and Cadmium Adsorption Characteristics of Selected Acid and Calcareous Soils. Soil Sci. Soc. Am. J. 42: 550-556.

Chao, T. T. 1984. Use of Partial Dissolution Techniques in Geochemical Exploration. J. Geochem. Explor. 20: 101-135.

Chen, Ming; Ma, Lena Q; Harris, Willie G. 1999. Baseline Concentrations of 15 Trace Elements in Florida Surface Soils. J. Environ. Qual. 28: 1173-1181.

Chlopecka, A. 1993. Forms of Trace Metals from Inorganic Sources in Soils and Amounts Found in Spring Barley. Water Air Soil Pollut. 69: 127-134.

Chlopecka, A.; Bacon. J. R.; Wilson, M. J. and Kay, J. 1996. Forms of Cadmium, Lead, and Zinc in Contaminated Soils from Southwest Poland. J. Environ. Qual. 25: 69-79.

Davies, B. E. 1990. Lead. In Heavy metals in soils. Edited by B. J. Alloway. John Wiley and Sons, Inc. New York. Pp. 177-196.

Davis, J. A. and Leckie, J. O. 1978a. Surface Ionization and Compelxation at the Oxide/Water Interface. II. Surface Properties of Amourfous Iron Oxyhydroxide and Adsorption of Metal Ions. J. Coll. Interf. Sci. 67: 90-107.

Davis, J. A. and Leckie, J. O. 1978b. Effect of Adsorbed Complexing Ligands on Trace Metal Uptake by Hydrous Oxides. Environ. Sci. Technol. 12: 1309-1315.

Davis, J. A. and Leckie, J. O. 1979. Speciation of Adsorbed Inos at the Oxide/Aqueous Interface. In Chemical Modeling in Aqueous Systems. Edited by Jenne, E. A. ACS Symposium Series. No. 93. American Chemical Society, Washington, D.C. Pp. 299-317.

Davis, J. A. and Leckie, J. O. 1980. Surface Ionization and Compexation at the Oxide/Water Interface. 3. Adsorption of Anions. J. Coll. Interf. Sci. 74: 32-43.

Davis, J. A. James, R. O. and Leckie, J. O. 1978. Surface Ionization and Complexation at the Oxide/Water Interface. 1. Computation of Electrical Double Layer properties in Simple Electrolytes. J. Coll. Interf. Sci. 63: 480-499.

Dzombak, D. A. 1986. Toward a Uniform Model for the Sorption of Inorganic ions on Hydrous Oxides. Ph. D. thesis, Massachusetts Institute of Technology, Cambridge, Mass.

Dzombak, D. A. and Morel, F. M. 1986. Sorption of Cadmium on Hydrous Ferric Oxide at High Sorbate/Srorbent Ratios: Equilibrium, Kinetics and Modeling. J. Coll. Interf. Sci. 112: 588-598.

Dzombak, D. A. and Morel, F. M. 1987. Adsorption of Inorganic Pollutants in Aquatic Systems. J. Hydraulic Engr. 113: 430-475.

Dzombak, D. A. and Morel, F. M. 1990. Surface Complexation Modeling; Hydrous Ferric Oxide. 1st edition. John Wiley & Sons, New York, NY, United States (USA). Pp. 393.

Elliott, HA; Liberati, MR; Huang, CP. 1986. Effect of Iron Oxide Removal on Heavy Metal Sorption by Acid Subsoils. Water Air Soil Pollut. 27 (3-4): 379-389.

Farley, K. J.; Dzombak, D. A.; and Morel, F. M. 1985. A Surface Precipitation Model for the Sorption of Cations on Metal Oxides. J. Coll. Interface Sci. 106: 226-242.

Fu, G.; Allen, H. E. and Cowan, C. E. 1991. Adsorption of Cadmium and Copper by Manganese Oxide. Soil Sci. 152:72-81.

Fulghum, J. E., Bryan, S. R. and Linton, R. W. 1988. Discrimination Between Adsorption and Co Precipitation in Aquatic Particle Standards by Surface Analysis Thechiques: Lead Distributions in Calcium Carbonates. Environ. Sci. Technol. 22: 463-467.

Fuller, W. H.; Korte, E. E.; Niebla, E. E.; and Alesii, B. A. 1976. Contribution of the

Soil to the Migration of Certain Common Trace Elements. Soil Sci. 122 (4): 223-234.

Garrels, R. M. and Christ, C. L. 1965. Solutions, Minerals, and Equilibria. Freeman, Cooper and Co. Harper & Row, New York. Pp. 450.

Gee, G. W. and Bauder, J. W. 1996. Particle-size Analysis. In Methods of Soil Analysis. Part 1, 3ed. Physical and Mineralogical Methods. Edited by Sparks, D. L. et. al. Soil Science Society of America and American Society of Agronomy, Madison, WI. Pp. 377-382.

Gilkes, R. 1994. Transmission Elecrton Microscope Analysis of Soil Materials. In Quantitative Methods in Soil Mineralogy. Segoe Rd. Soil Science Society of America. Madison, WI. Pp. 177-204.

Goldberg, E. 1954. Chemical scavengers of the sea, Part 1 of Marine geochemistry. Journal of Geology. 62 (3): 249-265.

Goldberg, S. 1995. Adsorption Models Incorporated into Chemical Equilibrium Models. In Chemical Equilibrium and Reaction Models. Edited by Loeppert, R. H. et al. Soil Sci. Soc. Am. J. Madison, WI. Pp. 75-95.

Goldberg, S; Forster, H. S.; and Godfery. C. L. 1996. Molybdenum adsorption on oxides, clay minerals, and soils. Soil Sci. Soc. Am. J. 60 (2): 425-432.

Harmsen, K. 1977. Behavior of Heavy Metal in Soils. Agric. Res. Report 866, Center for Agric. Pupilshing and Documentation Wageningen, Netherlands. Pp. 171.

Harvey, D. T. and Linton, R. W. 1984. X-Ray Photoelectron Spectroscopy (XPS) of Adsorbed Zinc on Amorphous Hydrous Ferric Oxide. Colloids and Surfaces. 11: 81-96.

Hayes, K. F. 1987. Equilibrium, Spectroscopic, and Kinetic Studies of Ion Adsorption at the Oxide/Aqueous Interface. Ph. D. Dissertation, Stanford University.

Hickey, M.G. and Kittrick, J.A. 1984. Chemical Partitioning of Cd, Cu, Ni and Zn in Soils and Sediments Containing High Levels of Heavy Metals. J. Environ. Qual. 13: 372-376.

Holm, P. E., Andersen, B. B., and Christensen, T. H. 1996. Cadmium Solubility in Aerobic soils. Soil Sci. Soc. Am. J. 60: 775-780.

Hossner, L.R. 1996. Dissolution for Total Methods of Soil Analysis Elemental Analysis. In Methods of soil analysis. Part 3, 3^{ed}. Chemical Methods. Edited by Sparks, D. L. et al. Soil Science Society of America and American Society of Agronomy, Madison, WI. Pp: 46-64.

Huang, C. P. and Stumm, W. 1973. Specific adsorption of cations on hydrous γ-Al_2O_3. J Colloid Interface Sci. 43: 409-420.

Jackson, M. L. 1956. Soil Chemical Analysis Advanced Course. Madison, WI.

Jenne, J. E. 1968. Control on Mn, Fe, Co, Ni, Cu and Zn Concentrations in Soils and Water: The Significant Role of Hydrous Mn and Fe Oxides. In Trace Inorganics in Water. Edited by Gould, R. F. Adv. Chem. Ser. 73. Am. Chem. Soc., Washington, D. C. 337-387.

Karlsson, S.; Allard, B.; and Hakansson, K. 1988. Chemical Characterization of Sstream-Bed Sediments Receiving High Loadings of Acid Mine Effluents. Chemical Geology. 67: 1-15.

Kinnibrugh, D. G.; Jackson, M. L.; and Syers, J. K. 1976. Adsorption of Alkaline Earth, Transition, and Heavy metals Cations by Hydrous Oxide Gels of Iron and

Alumimium. Soil Sci. Soc. Am. J. 40: 796-799.

Klages, M. G. and Hopper, W. R. 1982. Clay Minerals in Northern Plains Coal Overburden as Measured by X-ray Diffraction. Soil Sci. Soc. Am. J. 46: 415-419.

Kookana, R. S.; Naidu, R.; Barry, D. A. Tran, Y. T. and Bajracharya, K. 1999. Sorption-Desorption Equilibria and Dynamics of Cadmium During Transport in Soil. In, Fate and Transport of Heavy Metals in the Vadose Zone. Edited by Selim, M. and Iskandar, K. First edition. Lewis Publishers. Pp.59-90.

Kornicker, W. A., Morse, J. W. and Damascenos, R. N. 1985. The chemistry of Co Interaction With Calcite and Aragonite Surfaces. Chem. Geol. 53: 229-236.

Krauskopf, K. B. 1956. Factors Controlling the Concentrations of Thirteen Rare Metals in Sea-Water. Geochim. Cosmochim. Acta. 9 (1-2): 1-32.

Kunze, G.W. and Dixon, J.B. 1994. Pretreatment for Mineralogical Analysis. In Methods of soil analysis. Part 1, 2ed. Physical and Mineralogical Methods. Edited by Sparks, D. L. et al. Soil Science Society of America and American Society of Agronomy, Madison, WI.

Kuo, S; Heilman, PE; Baker, AS. 1983. Distribution and Forms of Copper, Zinc, Cadmium, Iron, and Manganese in Soils near a Copper Smelter. Soil Sci. 135 (2): 101-109.

Levy, D. B.; Barbarick, K. A.; Siemer, E. G.; and Sommers, L. E. 1992. Distribution and Partitioning of Trace Metals in Contaminated Soils near Leadville, Colorado. J. Environ. Qual. 21: 185-195.

Lindsay, W. 1979. Chemical equilibrai in soils. 1st edition. A Wiley-Interscience Publication. John Wiley and Sons, New York.

Loeppert, R. H. and Inskeep, W. P. 1996. Iron. In Methods of soil analysis. Part 3, 3ed edition. Chemical Methodes. Edited by Sparks, D. L. et al. Soil Science Society of America and American Society of Agronomy, Madison, WI. Pp. 639-664.

Loeppert, R. H. and Suarez, D. 1996. Carbonate and Gypsum. In Methods of Soil Analysis. Part 3, 3ed edition. Chemical Methods. Edited by Sparks, D. L. et al. Soil Science Society of America and American Society of Agronomy, Madison, WI. Pp. 437-474.

McBride, M. B. 1989. Reactions Controlling Heavy Metal Solubility in Soils. In Advances in Soil Science Volume 10. Edited by Stewart, B. A. Springer-Verlag Inc. New York. Pp. 1-56.

McBride, M. B. and Blasiak, J. J. 1979. Zinc and Copper Solubility as a Function of pH in an Acid Soil. Soil Sci. Soc. Am. J. 43: 866-870.

McBride, M. B. Fraer, A. R. and McHardy, W. J. 1984. Cu^{2+} Interaction with Microcrystalline Gibbsite. Evidence for Oriented Chemisorbed Copper Ions. Clays and Clay Minerals. 32: 12-18.

McBride, M., Sauve, S., and Hendershot, W. 1997. Solubility Control of Cu, Zn, Cd and Pb in Contaminated soil. European Journal of Soil Science. June 48: 337-346.

McKenzie, R.M. 1980. The Adsorption of Lead and Other Heavy Metals on Oxides of Manganese and Iron. Aust. J. Soil Res. 18: 61-73.

Moore, D. M. and Reynolds, R. C. 1997. X-Ray Diffraction and the Identification and

Analysis of Clay Minerals. 2nd edition. Oxford New York, Oxford University Press. Pp. 378.

Moore, D. W. Ficklin, W. H. and Carolyn, J. 1988. Partitioning of Arsenic and Metals in Reducing Sulfidic Sediments. Environ. Sci. Technol. 22: 432-437.

Nelson, D. W. and Sommers, L. E. 1996. Total Carbon, Organic Carbon, and Organic Matter. In Methods of soil analysis. Part 3, 3ed. Chemical Methods. Edited by Sparks, D. L. et. al. Soil Science Society of America and American Society of Agronomy, Madison, WI. Pp. 961-1010.

Papadopoulos, P. and D. L. Rowell. 1988. The Reactions of Cadmium and Zinc with Calcium Carbonate Surfaces. J. Soil Sci. 39: 23-36.

Pardo, M.T. 1997. Influence of Electrolyte on Cadmium Interaction with Selected Andisols and Alfisols. Soil Sci. 162 (10): 733-740.

Parkman, H. R., Charnock, J. M., Livens, F. R., and Vaughan, D. J. 1998. A Study of the Interaction of Strontium Ions in Aqueous Solution with The Surfaces of Calcite and Kaolinite. Geochim. Cosmochim. Acta. 62 (9): 1481-1492.

Ramos, L.; Hernandez, L. M.; and Gonzalez, M. J. 1994. Sequential Fractionation of Copper, Lead, Cadmium and Zinc in Soils from Near Donana National Park. J. Environ. Qual. 23: 50-57.

Saeed, M. and Fox, R. L. 1979. Influence of Phosphate Fertilization on Zinc Adsorption by Tropical Soils. Soil Sci. Soc. Am. J. 43: 683-686.

Santillan-Medrano, J. and Jurinak. 1975. The chemistry of Lead and Cadmium in Soil: Solid Phase Formation. Soil Sc. Soc. Am. Proc. 39: 851-856.

Sauve, S.; Martinez, C. E.; McBride, M.; and Hendershot, W. 2000. Adsorption of Free Lead by Pedogenic Oxides, Ferrihydrite, and Leaf Compost. Soil Sci. Soc. Am. J. 64: 595-599.

Sawhney, B. L. 1986. Electron Microprobe Analysis. In Methods of soil analysis. Part 1, Physical and Mineralogical. 2nd. Edited by Klute, Arnold. Pp. 271-290. Soil Science Society of America and American Society of Agronomy, Madison, WI.

Schenck, C. V.; Dillard, J. C. and Murray, J.W. 1983. Surface Analysis and the Adsorption of Co^{2+} on Goethite. J. Coll. Interf. Sci. 95: 398-409.

Schwertmann, U. and Cornell, M. R. 2000. Iron Oxides in the Laboratory, Preparation and Characterization. 2nd Edition. Wiley-VCH Verlag GmbH, Weinheim. Pp. 188.

Schwertmann, U. and Taylor, R. M. 1989. Iron Oxides. In Minerals in Soil Environments (2nd edition). Edited by Dixon, J. and Weed, S. Soil Science Society of America, Madison, WI, USA. Pp: 379-438.

Shuman, L. M. 1988. Effect of Removal of Organic Matter and Iron of Manganese Oxides on Zinc Adsorption by Soil. Soil Sci. 146: 248-254.

Singh, Bijay and Sadana, U. S. 1987. Behavior of Toxic Elements in the Soil-Plant System and Associated Hazards in Intensive Agriculture. Annals of Biology. 3 (1) :1-14.

Song, Y.; Wilson, M. J.; Moon, H. S.; Bacon, J. R.; and Bain, D. C. 1999. Chemical and Mineralogical Forms of Lead, Zinc and Cadmium in Particle Size Fractions of Some Wastes, Sediments and Soils in Korea. Applied Geochemistry. 14: 621-633.

Sposito, G.; Lund, L. J.; and Chang, A. X. 1982. Trace Metal Chemistre in Arid-zone Soils Amended with Sewage Sludge. 1. Fractionations of Ni, Cu, Zn, Cd and Pb in Solid Phases. Soil Sci. Soc. Am. J. 46: 260-264.

Sposito, Garrison. 1989. The Chemistry of Soils. Oxford University press, Oxford. Pp. 277.

Stumm, W. and Morgan, J. 1981. Aquatic Chemistry. New York: Wiley.

Stumm, W. and Morgan. J. 1996. Aquatice Chemistry: Chemical Equilibria and Rates in Natural Waters. Willy & Sons, New York. Pp. 1022.

Stumm, W.; Huang, C. P.; and Jenkins. S. R. 1970. Specific Chemical Interaction Affecting the Stability of Dispersed Systems. Croatica Chim. Acta, V. 42: 223-245.

Tessier, A.; Campbell, P. G.; and Bisson, M. 1979. Sequential extraction procedure for the speciation of particulate trace metals. Anal. Chem. 51 (7): 844-850.

Tewari, P. H. and Lee, W. 1975. Adsorption of Co^{2+} at the Oxide-Water Interface. J. Coll. Interf. Sci. 52: 77-88.

Thomas, G. W. 1996. Soil pH and Soil Acidity. In Methods of soil analysis. Part 3, Chemical Methods. 3^{ed}. Edited by Sparks, D. L. et. al. Soil Science Society of America and American Society of Agronomy, Madison, WI. Pp. 475-490

Tiller, K. G., J. Geith, and G. Brummer. 1984a. The Sorption of Cd, Zn and Ni by a Soil Clay Fraction: Procedures for Partion of Bound Forms and their Interpretation. Geoderma 34: 1-16.

Tiller, K. G., J. Geith, and G. Brummer. 1984b. The Relative Affinities of Cd, Ni, and Zn for Different Soil Clay Fractions Geothie. Geoderma 34: 17-35.

Whittig, L. D. and Allardice, W. R. 1994. X-Ray Diffraction Techniques. In Methods of Soil Analysis. Part 1, 2^{ed} edition. Physical and Mineralogical Methods. Edited by Klute, A. Soil Science Society of America and American Society of Agronomy, Madison, WI. 331-362.

Williams, D. B. and Carter, C. B. 1996. Transmission Electron Microscopy. A Division of Plenum Publishing Corporation. New York. Pp. 729.

Wu, J., Laird, D. A., and Thompson, M. L. 1999. Sorption and Desorption of Copper on Soil Clay Components. J. Environ. Qual. 28: 334-338.

Xian, X. 1987. Chemical partitioning of Cd, Zn, Pb, and Cu in Soils Near Smelter. Journal of environmental science and health. Part A. Environmental Science and Engineering. 22: 527-514.

Xu, Y., Schwartz, F. W., and Traina, S. J. 1994. Sorption of Zn^{2+} and Cd^{2+} on Hydroxyapatite Surfaces. Environ. Sci. Technol. 28: 1472-1480.

Yarlagadda, P. S. Matsumoto, M. R. Van Benschoten, J. E. and Kathuria, A. 1995. Characteristics of Heavy Metals in Contaminated Soils. Journal of Environmental Engineering. 121 (4): 276-286.

Appendix 1: XRD analysis of clay fraction of the soil sample at a depth of 5-10 cm; K treatment K 550°C; Mg; and Mg-EG.

Mineral	K				K 550°C				Mg				Mg, EGME			
	Position		I	Area	Position		I	Area	Position		I	Area	Position		I	Area
	Deg.	DSp.			Deg.	DSp.			Deg.	DSp.			Deg.	DSp.		
Vermiculite									6.14	14.4	52.5	1930	5.37	16.4	51.4	0
Illite	8.83	10.0	89.2	4590	8.87	9.96	69.8	4740	8.86	9.97	62.8	2310	8.84	10.0	66.7	2740
Kaolinite	12.4	7.15	62.3	3210					12.4	7.13	64.4	2370	12.4	7.15	55.1	2260
									15.1	5.85	37.4	1200	15	5.92	19.3	0
Illite	17.8	4.99	47.2	2430	17.7	5.00	36.3	2470	17.9	4.96	51.6	1890	17.8	4.97	37.5	0
					19.8	4.48	9.93	0	19.7	4.51	27.0	992	19.7	4.51	35.3	0
Quartz	20.9	4.25	21.3	1100	20.9	4.24	13.6	0	20.8	4.26	20.1	0	20.9	4.25	26.8	0
									22.9	3.88	26.7	857	22.9	3.88	26.2	0
	23.8	3.74	18.8	969									24.9	3.57	48.2	0
Kaolinite	24.9	3.57	60.8	2740					24.9	3.57	58.8	1890				
I&Q	26.7	3.34	100	5150	26.7	3.34	100	6790	26.7	3.34	100	3670	26.7	3.34	100	4110
	28.4	3.14	72.2	2790												

Appendix 2: XRD analysis of clay fraction of the soil sample at a depth of 10-15 cm; K treatment K 550°C; Mg; and Mg-EG.

Mineral	K				K 550°C				Mg				Mg, EGME			
	Position		I	Area	Position		I	Area	Position		I	Area	Position		I	Area
	Deg.	DSp.			Deg.	DSp.			Deg.	DSp.			Deg.	DSp.		
Vermiculite									6.27	14.1	27.8	0				
Illite	8.82	10.0	83.3	6580	8.90	9.93	64.6	6230	8.90	9.93	78.9	6650	8.88	9.95	69.5	5600
Kaolinite	12.4	7.16	62.0	4890					12.4	7.11	73.3	6170	12.4	7.13	66.0	5320
Illite	17.7	5.00	31.2	1850	17.8	4.97	21.7	2100	17.8	4.98	32.5	2740	17.8	4.97	32.1	0
Quartz	20.9	4.26	16.5	1140	21	4.24	16.3	1180	21	4.24	16.1	1020	20.9	4.26	18.5	0
Kaolinite	24.9	3.58	57	3940					25	3.56	70.3	5180	24.9	3.57	63.9	4500
I&Q	26.7	3.34	100	7890	26.7	3.33	100	9640	26.8	3.33	100	8420	26.7	3.34	100	8056

Appendix 3: XRD analysis of clay fraction of the soil sample at a depth of 15-20 cm; K treatment K 550°C; Mg; and Mg-EG.

Mineral	K				K 550°C				Mg				Mg, EGME			
	Position		I	Area	Position		I	Area	Position		I	Area	Position		I	Area
	Deg.	DSp.			Deg.	DSp.			Deg.	DSp.			Deg.	DSp.		
Vermiculite									6.11	14.5	57.8	4030	5.32	16.6	66.3	4480
Illite	8.84	10.0	100	5770	8.86	9.97	91.5	6100	8.86	9.97	100	6980	8.83	10.0	96	6480
Kaolinite	12.4	7.14	37.4	2160					12.4	7.14	57.4	4000	12.4	7.16	50.5	3400
									15.1	5.86	24.5	1710	15.1	5.87	15	0
Illite	17.8	4.99	48.3	2790	17.77	4.99	42.1	2810	17.8	4.98	64.6	4510	17.8	4.99	54.9	3700
Quartz	20.9	4.25	11.6	0	20.91	4.25	16.2	0	20.9	4.25	14.1	737	20.9	4.26	13.4	0
	21.4	4.16	12.0	0												
													23.8	3.74	15	0
Kaolinite	24.9	3.57	32.5	1870					24.9	3.57	45.7	3190	24.9	3.58	46.3	3120
I&Q	26.8	3.33	98.1	5650	26.67	3.34	100	6660	26.8	3.33	92.7	6470	26.7	3.34	100	6750
	28.4	3.14	43.5	2510												

Appendix 4: X-ray powder diffraction analysis of sand and silt fractions of the soil sample at a depth of of 5-10 cm.

Mineral	Sand				Silt			
	Position		I	Area	Position		I	Area
	Deg.	DSp.			Deg.	DSp.		
	8.91	9.92	3.09	810	8.88	9.95	7.29	1330
					12.4	7.15	4.31	0.00
	17.8	4.98	1.56	0.00	17.8	4.99	3.47	0.00
	19.7	4.49	1.77	0.00	19.8	4.48	4.36	0.00
Quartz	20.9	4.24	27.9	4190	20.9	4.25	25.9	2700
Orthoclase	21.1	4.22	3.79	0.00				
	22.1	4.02	2.92	875	22.1	4.02	4.94	516
Orthoclase	23.6	3.76	2.65	695				
	24.3	3.65	2.48	0.00				
	25.7	3.46	2.36	0.00				
Quartz	26.7	3.34	100	15000	26.7	3.34	100	10400
Orthoclase	26.9	3.31	6.96	1040	26.9	3.31	11.6	1210
Orthoclase	27.2	3.28	2.98	782				
	27.5	3.24	3.67	1100	27.5	3.24	6.21	1333
	27.8	3.20	6.31	142				
	28	3.19	6.21	1400	28	3.19	9.47	1480
					33.1	2.70	2.06	0.00
					35.0	2.56	3.95	0.00
Quartz	36.6	2.45	7.00	1570	36.6	2.45	9.80	1540
Quartz	39.5	2.28	6.91	1300	39.5	2.28	6.49	848
Quartz	40.4	2.23	3.87	869	40.4	2.23	4.44	812
Quartz	42.5	2.12	8.66	1620	42.5	2.13	6.77	1060
					45.5	1.99	3.33	0.00
Quartz	45.9	1.98	4.69	879	45.8	1.98	5.60	1020
Quartz	50.2	1.82	15.4	2880	50.2	1.82	12.4	1620
	50.6	1.80	3.37	1010				
Quartz	54.9	1.67	3.83	861	54.9	1.67	3.90	0.00
Quartz	60.0	1.54	8.17	2140	60	1.54	8.78	1600
	64.1	1.45	2.40	0.00	64.1	1.45	2.50	0.00

Appendix 5: X-ray powder diffraction analysis of sand and silt fractions of the soil sample at a depth of 10-15 cm.

Mineral	Sand				Silt			
	Position		I	Area	Position		I	Area
	Deg.	DSp.			Deg.	DSp.		
	8.90	9.93	10.1	1700	8.91	9.92	4.34	1210
					12.4	7.13	1.85	0.00
	13.7	6.44	1.55	0.00	13.9	6.36	1.50	0.00
	17.8	4.97	1.84	0.00	17.9	4.96	2.30	0.00
	19.8	4.47	1.45	0.00	19.9	4.46	2.81	0.00
Quartz	20.9	4.25	30	5060	20.9	4.24	20.1	3500
Micr. & O	21.1	4.21	3.69	312	21.1	4.20	4.04	0.00
	22.1	4.02	1.79	0.00	22.1	4.02	4.60	961.8
	22.4	3.97	1.55	0.00	23.7	3.76	4.10	857.5
	22.7	3.91	1.21	0.00				
Micr. & O	23.6	3.77	2.24	378				
	24.3	3.67	2.18	552	24.3	3.66	2.81	0.00
					25.5	3.50	3.14	0.00
	25.6	3.48	4.20	709	25.7	3.47	2.93	0.00
Quartz	26.7	3.34	100	21100	26.7	3.33	100	13900
Orthoclaze	26.9	3.31	8.15	1030	26.9	3.31	10.9	1140
Micr. & O	27.1	3.29	2.92	615.00	27.1	3.29	4.12	862
					27.2	3.28	4.01	1120
Microcline	27.5	3.24	24.5	6196	27.6	3.24	7.00	1710
	27.7	3.22	3.78	958	27.8	3.20	6.74	1881
	27.8	3.21	3.39	1150				
	28	3.18	4.93	1460	28.0	3.18	10.2	2140
	28.3	3.15	3.19	1080				
	34.4	2.61	1.45	0.00				
	35	2.57	1.87	0.00	35	2.56	2.75	0.00
					35.1	2.56	3.12	0.00
	35.8	2.50	1.54	0.00				
Quartz	36.6	2.45	8.28	1400	36.6	2.45	9.12	1600
Quartz	39.5	2.28	13.3	2800	39.6	2.28	6.18	1290

Appendix 5 cont.

Mineral	Sand				Silt			
	Position		I	Area	Position		I	Area
	Deg.	DSp.			Deg.	DSp.		
Quartz	40.3	2.23	4.24	896	40.4	2.23	3.64	762
Quartz	42.5	2.13	7.44	15700	42.5	2.12	6.75	1180
	45.3	2.00	1.89	0.00	45.5	1.99	1.85	0.00
Quartz	45.8	1.98	3.75	792	45.9	1.98	3.98	971
Quartz	50.2	1.82	8.03	1690	50.2	1.82	9.32	1620
	50.6	1.80	2.40	607				
Quartz	54.9	1.67	4.22	1070	54.9	1.67	3.98	832
Quartz	55.3	1.66	1.95	0.00	55.4	1.66	2.14	0.00
Quartz	60.0	1.54	7.89	1664	60.0	1.54	8.58	1790
					62.6	1.48	1.60	0.00
					64.1	1.45	2.21	0.00

Appendix 6: X-ray powder diffraction analysis of Clay Untreated Chemically; Silt and sand Untreated Chemically; sand; and silt fractions of the soil sample at a depth of 15-20 cm.

Mineral	Clay Untreated Chemically				Silt and sand Untreated Chemically				Silt				Sand			
	Position		I	Area	Position		I	Area	Position		I	Area	Position		I	Area
	Deg.	DSp.			Deg.	DSp.			Deg.	DSp.			Deg.	DSp.		
Vermiculite	6.22	14.2	38.7	899												
Illite	8.92	9.90	39.1	907	8.93	9.89	2.44	0.00	8.83	10.0	10.2	1870	8.93	9.89	2.44	0.00
Kaolinite	12.4	7.12	25.5	0.00					12.4	7.11	2.35	0.00				
	15	5.92	18.7	0.00												
Illite	17.9	4.96	29.9	0.00					17.8	4.99	4.25	777				
Illite	19.9	4.46	40.6	943					19.9	4.46	3.66	0.00				
Quartz					21	4.25	19.1	0.00								
					21	4.23	19.1	1851	20.9	4.25	22.9	3489	20.9	4.25	19.1	0.00
Geothite	21.3	4.16	41.7	970					21.0	4.22	4.47	0.00	21	4.23	19.1	1850
					22.2	4.00	10.1	786	22.1	4.03	3.87	0.00	22.2	4.00	10.1	786
					23.0	3.86	6.03	701					23.0	3.86	6.03	701
					23.4	3.81	9.17	534					23.4	3.81	9.17	534
					23.7	3.75	5.41	630	23.5	3.78	3.23	0.00	23.7	3.75	5.41	630
					24.2	3.68	7.23	701	24.3	3.67	3.10	0.00	24.2	3.68	7.23	701
					25.7	3.46	10.5	813	25.6	3.48	3.70	0.00	25.7	3.46	10.5	813
I & Q	26.7	3.33	100	2030	26.7	3.34	100	11640	26.7	3.34	100	15200	26.7	3.34	100	11640
					27.1	3.28	5.05	685	27.0	3.30	4.09	873	27.1	3.28	5.05	685
					27.5	3.24	6.19	961	27.5	3.24	3.94	960	27.5	3.24	6.19	961
									27.8	3.21	5.10	1240				
					28	3.19	7.10	1100	27.9	3.19	6.63	1610	28	3.19	7.10	1100
	29.1	3.07	29.2	0.00												
									29.9	2.99	3.66	781				
Geothite	33.2	2.70	26.9	0.00												
	35.1	2.56	38.1	884	35.2	2.55	3.09	0.00	35.1	2.56	3.74	0.00	35.2	2.55	3.09	0.00
Quartz	36.7	2.45	36	0.00	36.6	2.45	20.4	1980	36.6	2.46	8.37	1530	36.6	2.45	20.4	1980

Appendix 7: X-ray powder diffraction analysis of Clay Untreated Chemically; Silt and sand Untreated Chemically; sand; and silt fractions of soil sample at depth 15-20.

Mineral	Clay Untreated Chemically				Silt and sand Untreated Chemically				Silt				Sand			
	Position		I	Area	Position		I	Area	Position		I	Area	Position		I	Area
	Deg.	DSp.			Deg.	DSp.			Deg.	DSp.			Deg.	DSp.		
Vermiculite	6.22	14.2	38.7	899												
Illite	8.92	9.90	39.1	907	8.93	9.89	2.44	0.00	8.83	10.0	10.2	1870	8.93	9.89	2.44	0.00
Kaolinite	12.4	7.12	25.5	0.00					12.4	7.11	2.35	0.00				
	15	5.92	18.7	0.00												
Illite	17.9	4.96	29.9	0.00					17.8	4.99	4.25	777				
Illite	19.9	4.46	40.6	943					19.9	4.46	3.66	0.00				
Quartz					21	4.25	19.1	0.00								
					21	4.23	19.1	1851	20.9	4.25	22.9	3489	20.9	4.25	19.1	0.00
Geothite	21.3	4.16	41.7	970					21.0	4.22	4.47	0.00	21	4.23	19.1	1850
					22.2	4.00	10.1	786	22.1	4.03	3.87	0.00	22.2	4.00	10.1	786
					23.0	3.86	6.03	701					23.0	3.86	6.03	701
					23.4	3.81	9.17	534					23.4	3.81	9.17	534
					23.7	3.75	5.41	630	23.5	3.78	3.23	0.00	23.7	3.75	5.41	630
					24.2	3.68	7.23	701	24.3	3.67	3.10	0.00	24.2	3.68	7.23	701
					25.7	3.46	10.5	813	25.6	3.48	3.70	0.00	25.7	3.46	10.5	813
I & Q	26.7	3.33	100	2030	26.7	3.34	100	11640	26.7	3.34	100	15200	26.7	3.34	100	11640
					27.1	3.28	5.05	685	27.0	3.30	4.09	873	27.1	3.28	5.05	685
					27.5	3.24	6.19	961	27.5	3.24	3.94	960	27.5	3.24	6.19	961
									27.8	3.21	5.10	1240				
					28	3.19	7.10	1100	27.9	3.19	6.63	1610	28	3.19	7.10	1100
	29.1	3.07	29.2	0.00												
									29.9	2.99	3.66	781				
Geothite	33.2	2.70	26.9	0.00												
	35.1	2.56	38.1	884	35.2	2.55	3.09	0.00	35.1	2.56	3.74	0.00	35.2	2.55	3.09	0.00
Quartz	36.7	2.45	36	0.00	36.6	2.45	20.4	1980	36.6	2.46	8.37	1530	36.6	2.45	20.4	1980

Appendix 7: EDX spectra of the soil Fe-oxide particle (particle 1). Peaks of elements are labeled.

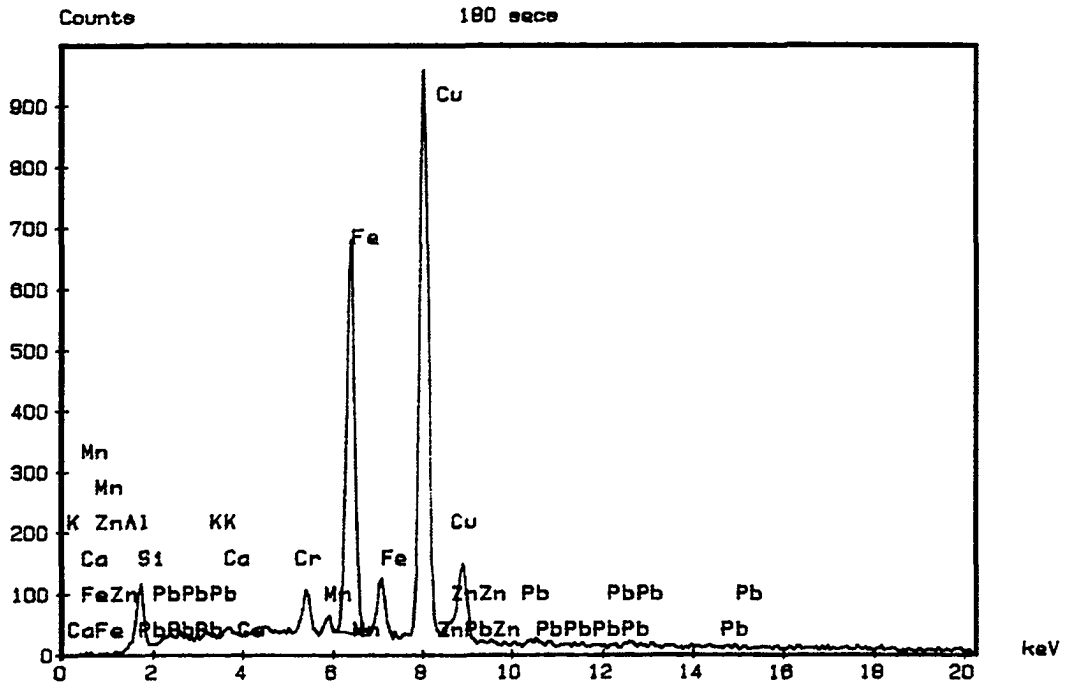

Appendix 8: EDX spectra of the soil Fe-oxide particle (particle 1). Peaks of elements are labeled.

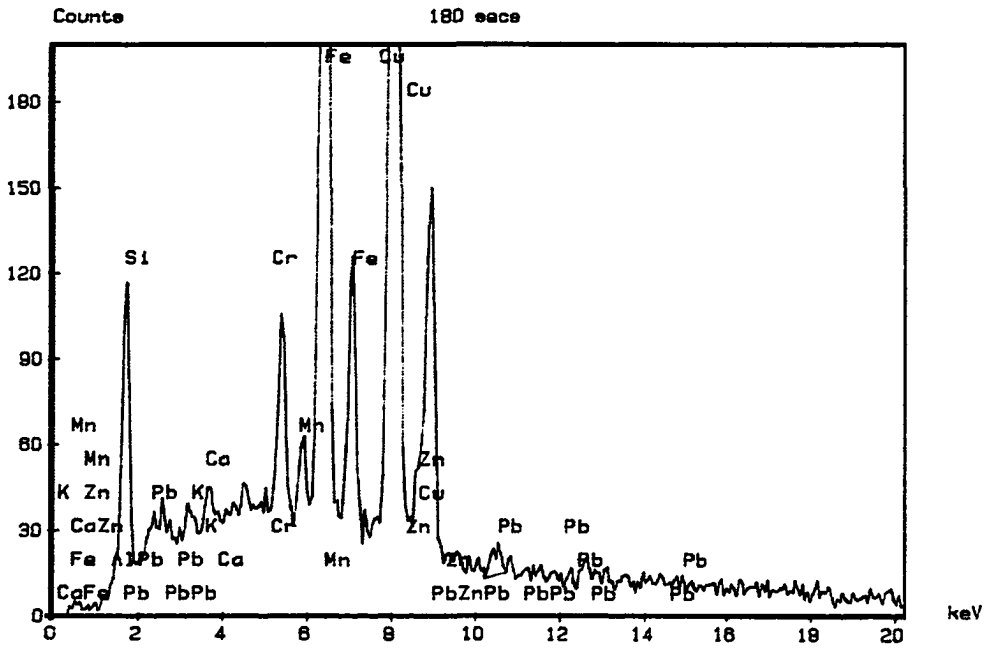

Appendix 9: EDX spectra of the soil Fe-oxide particle (particle 2). Peaks of elements are labeled.

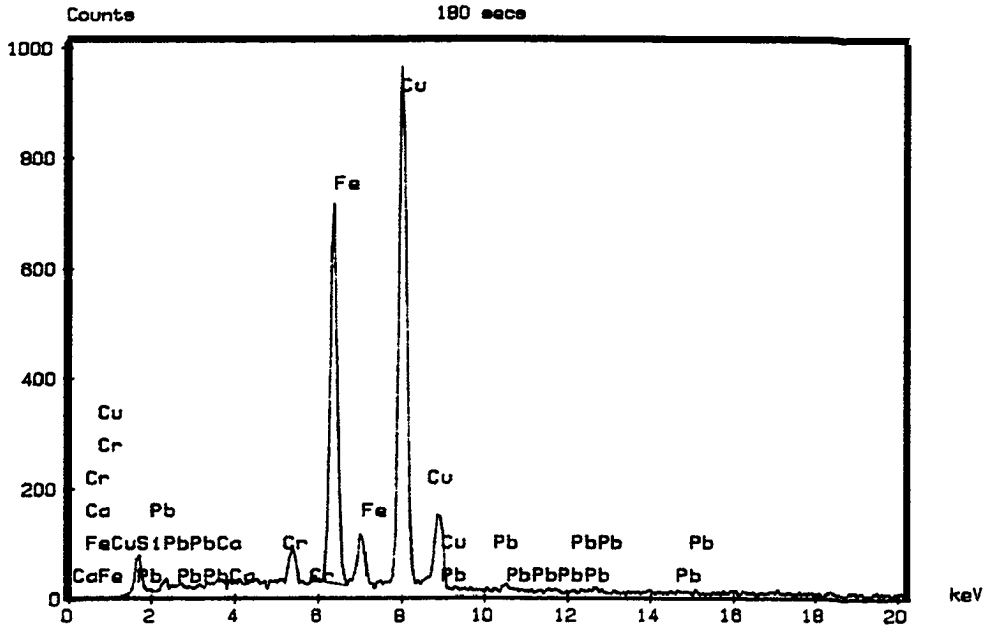

Appendix 10: EDX spectra of the soil Fe-oxide particle (particle 3). Peaks of elements are labeled.

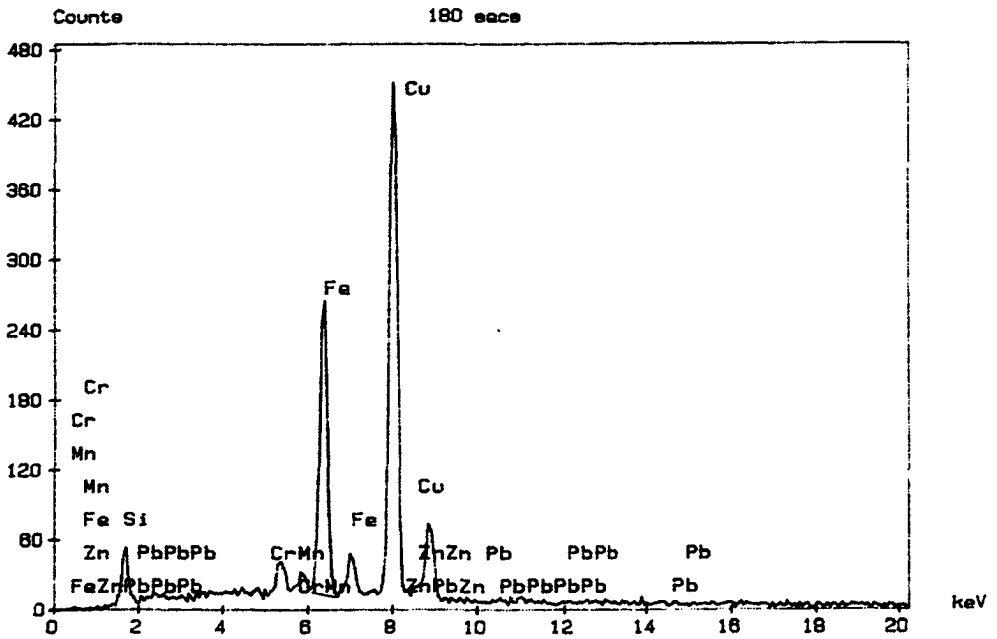

Appendix 11: EDX spectra of the soil Fe-oxide particle (particle 4). Peaks of elements are labeled.

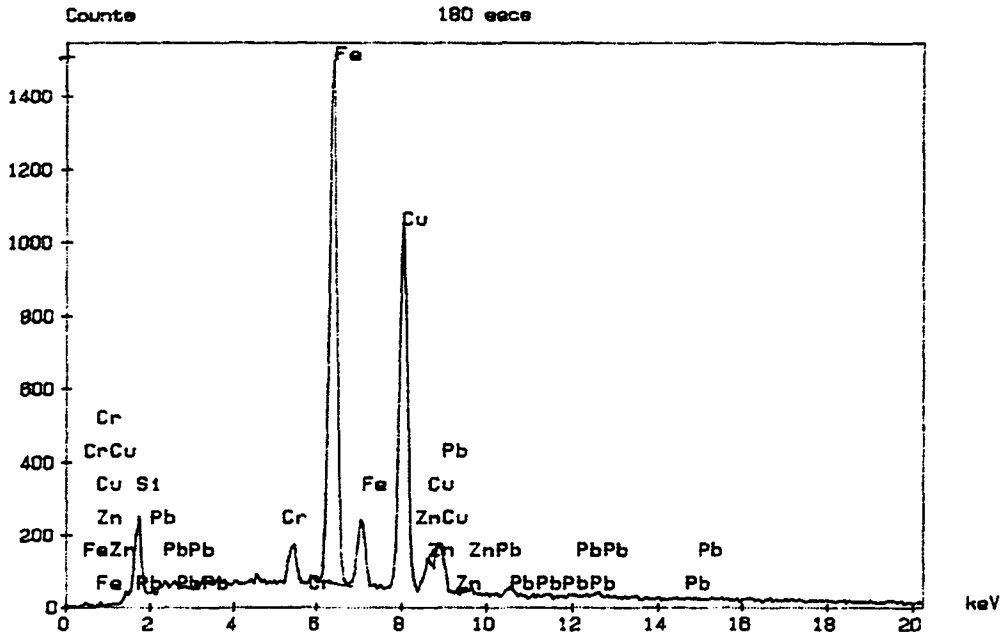

Appendix 12: EDX spectra of the soil Fe-oxide particle (particle 5). Peaks of elements are labeled.